Breach Volume Estimation of Tailings Storage Facility Failures

by

Niel Marais

"Thesis presented in fulfilment of the requirements for the degree of Master of Engineering in the Faculty of Engineering, at Stellenbosch University"

Supervisor: Dr Charles J. MacRobert

Department of Civil Engineering

March 2021

UNIVERSITEIT•STELLENBOSCH•UNIVERSITY
jou kennisvennoot • your knowledge partner

Plagiaatverklaring / *Plagiarism Declaration*

1 Plagiaat is die oorneem en gebruik van die idees, materiaal en ander intellektuele eiendom van ander persone asof dit jou eie werk is.
Plagiarism is the use of ideas, material and other intellectual property of another's work and to present is as my own.

2 Ek erken dat die pleeg van plagiaat 'n strafbare oortreding is aangesien dit 'n vorm van diefstal is.
I agree that plagiarism is a punishable offence because it constitutes theft.

3 Ek verstaan ook dat direkte vertalings plagiaat is.
I also understand that direct translations are plagiarism.

4 Dienooreenkomstig is alle aanhalings en bydraes vanuit enige bron (ingesluit die internet) volledig verwys (erken). Ek erken dat die woordelikse aanhaal van teks sonder aanhalingstekens (selfs al word die bron volledig erken) plagiaat is.
Accordingly, all quotations and contributions from any source whatsoever (including the internet) have been cited fully. I understand that the reproduction of text without quotation marks (even when the source is cited) is plagiarism.

5 Ek verklaar dat die werk in hierdie skryfstuk vervat my eie oorspronklike werk is en dat ek dit nie vantevore in die geheel of gedeeltelik ingehandig het vir bepunting in hierdie module/werkstuk of 'n ander module/werkstuk nie.
I declare that the work contained in this assignment is my original work and that I have not previously (in its entirety or in part) submitted it for grading in this module/assignment or another module/assignment.

NH Marais **Voorletters en van / *Initials and surname***	**March 2021** **Datum / *Date***

Declaration

By submitting this thesis electronically, I declare that the entirety of the work contained therein is my own original work, that I am the authorship owner thereof (unless to the extent explicitly otherwise stated) and that I have not previously in its entirety or in part submitted it for obtaining any qualification.

Date: March 2021

Dedication

I dedicate this thesis to my mother and father, thank you for your undying love and support throughout my academic career. To my sister, thank you for keeping me grounded and focussed on what really matters.

"You are, therefore, I am"- Thich Nhat Hanh

Further I would like to thank my supervisor, Dr. Charles MacRobert for his guidance and thought-provoking mentorship throughout the course of this project.

Abstract

Estimating the potential tailings release volume (V_F) and run-out distances (D_{max}) of Tailings Storage Facilities (TSFs) form an integral part of the Tailings Dam Breach Assessment (TDBA) process. These estimations largely rely on empirical relationships such as those suggested by Rico et al (2008), Concha & Lall (2018) and Quelopana (2019). These empirical relationships are functions of the TSFs geometric characteristics (height of the dam and total volume of the dam). Rourke & Luppnow (2015) assessed the effects of the supernatant pool present on the TSF prior to failure on the recorded outflow volume, a strong linear relationship was identified between the magnitude of failure and the pool ratio based on five failure cases which provided pool ratio data.

The aim of this thesis was to compile a database of recorded TSF failures that provided the TSF geometric characteristics mentioned above. The database of 56 failures was compiled from various literature sources, one such source is the World Mine Tailings Failure Database (WMTF) compiled by Bowker & Newman (2019). The main limitation encountered when compiling the failure database for analysis was the availability of recorded data, this was attributed to inaccurate or incomplete reporting of TSF failure data. The WMTF database contains more than 300 recorded failures dating back to 1915. The information contained in the database was then used to examine the relationships between the recorded TSF failures' geometric characteristics, recorded outflow volumes and run-out distances on a larger database with more failure cases. The relationships observed during the regression analysis phase of the thesis were then used to define four prediction models: two for estimating V_F and two for estimating D_{max} using Eureqa modelling software. The four models were defined as follows:

Model V_F.1: The first model defined for the estimation of V_F was modelled to be a function of the impoundment volume and height of a dam and utilized the full database of 56 failure cases. The aim was to develop a model that is comparable to the existing models. The resulting model performed better than the three existing models, achieving an R^2 value of 0.72 with a Root Mean Square Error (RMSE) of 1.207 Mm^3.

Model V_F.2: The second model defined for the estimation of V_F was modelled to be a function of the recorded pool ratio before failure, using 7 cases from the database which provided pool ratio data. The aim of developing this model was to improve the current model developed by Rourke & Luppnow (2015). The resulting model performed near identical to the existing one, achieving an R^2 value of 0.98 and a RMSE of 0.037 Mm^3. It is recommended that a study is completed looking specifically at the relationship between the pool ratio and saturation levels of the tailing material on the potential release volume.

Model D_{max}.1: The first model defined for the estimation of D_{max} was modelled using 37 cases from the database which presented recorded D_{max} values for the failures. The function was defined to incorporate the impoundment volume, release volume and height of the dam as the predictor variable Hf. The aim

was to develop a more accurate model than existing models. The model performed relatively well compared to the existing models of Rico et al (2008) and Concha Larrauri & Lall (2019), achieving a R^2 value of 0.81 with a RMSE of 47.72 km. This was attributed to the variance between values for both D_{max} and Hf. Additionally, D_{max} varies substantially between failures and is dependent on various external factors such as site topography, TSF proximity to a water course and possible natural or manmade barriers.

Model D_{max}.2: The second model defined for the estimation of D_{max} was modelled using the same 7 cases used for model V_F.2. In addition to the pool ratio, the gradient of the flow path was introduced as a variable. The gradient was taken from the center of the tailings dam to the lowest point along the flow path of the breached tailings material. The model performed relatively well, achieving a R^2 value of 0.77 and an RMSE of 3. The model, however, is very limited, again attributed to the small dataset available for analysis.

Overall, the models performed as expected, model V_F.1 performed the best and may be applicable as a first approximation for predicting potential downstream impacts of a TSF failure given its stability and accuracy over a larger dataset. The models developed to incorporate pool ratio data performed well but it is necessary to expand on the size of the dataset to provide a more accurate representation. They do, however, show a strong relationship between the size of the supernatant pond and the expected tailings release volume. When looking at the models predicting the run-out distance it is important to note the complexity of variables influencing the distance that the tailings may travel. Site specific investigations and modeling should be conducted to identify the most probable flow path that consider the presence and volume of vegetation, natural barriers, and buildings.

Keywords: Tailings; Failure; Breach volume.

Opsomming

Die voorspelling van die potensiële vrystellingsvolume (V_F) en uitloopafstand (D_{max}) van uitskotstoorgeriewe vorm ’n integrale deel van die assesseringsproses van uitskotdambreuke. Hierdie voorspellings berus grotendeels op die empiriese verhoudings soos voorgestel deur Rico et al (2008), Concha & Lall (2018) en Quelopana (2019). Hierdie empiriese verwantskappe is funksies van die geometriese eienskappe (hoogte en totale volume) van ’n dam. Rourke & Luppnow (2015) het die verhouding tussen die oppervlakwater van uitskotdamme voor die ineenstorting en die gevolglike aangetekende uitvloeivolume ondersoek. 'n Sterk lineêre verband is geïdentifiseer tussen die omvang van die ineenstorting en die poelverhouding, gebaseer op vyf ineenstortings wat inligting oor poelverhoudings verskaf het.

Die doel van hierdie tesis was om 'n databasis saam te stel van opgetekende uitskotdamineenstortings wat die bogenoemde geometriese eienskappe getoon het. Die databasis van 56 ineenstortings is saamgestel uit verskillende literatuurbronne, onder meer die *World Mine Tailings Failure Database* (WMTF) wat deur Bowker & Newman (2019) saamgestel is. Die vernaamste beperking op die samestelling van die ineenstortingsdatabasis vir ontleding was die beskikbaarheid van opgetekende data. Dit word toegeskryf aan onakkurate of onvolledige verslagdoening oor uitskotdamineenstortings. Die WMTF-databasis bevat meer as 300 opgetekende ineenstortings wat tot by 1915 strek. Die inligting in die databasis is vervolgens gebruik om die verwantskappe tussen die opgetekende uitskotdamineenstortings se geometriese eienskappe, uitvloeivolumes en uitloopafstande te vergelyk met dié van ’n groter databasis met meer ineenstortingsgevalle. Die verwantskappe wat waargeneem is tydens die regressieontledingsfase van die tesis is vervolgens gebruik om vier voorspellingsmodelle te definieer: twee vir die voorspelling van V_F en twee vir die voorspelling van D_{max} met behulp van Eureqa-modelleringsagteware. Die vier modelle is soos volg omskryf:

Model V_F.1: Die eerste model wat vir die beraming van V_F gedefinieer is, is gemodelleer as ’n funksie van die totale volume en hoogte van ’n dam en het die volledige databasis van 56 ineenstortingsgevalle gebruik. Die doel was om 'n model te ontwikkel wat vergelykbaar is met die bestaande modelle. Die gevolglike model het beter gevaar as die drie bestaande modelle en het ’n R^2-waarde van 0,72 en 'n wgk-afwyking van 1,207 Mm^3 behaal.

Model V_F.2: Die tweede model wat vir die beraming van V_F gedefinieer is, is gemodelleer as 'n funksie van die aangetekende poelverhouding voor ineenstorting, met behulp van 7 gevalle uit die databasis wat die poelverhoudingsdata verskaf het. Die doel van die ontwikkeling van hierdie model was om die huidige model wat deur Rourke & Luppnow (2015) ontwikkel is, te verbeter. Die model wat hieruit voortgevloei het, is amper identies aan die bestaande model en behaal ’n R^2-waarde van 0,98 en ’n wgk-afwyking van 0,037 Mm^3. Dit word aanbeveel dat ’n studie onderneem word om spesifiek te kyk na die

verband tussen die poelverhouding en versadigingsvlakke van die uitskotmateriaal en die potensiële vrystellingsvolume.

Model D_{max}.1: Die eerste model wat vir die beraming van D_{max} gedefinieer is, is gemodelleer deur gebruik te maak van 37 gevalle uit die databasis wat die opgeneemde D_{max}-waardes vir die ineenstortings aangebied het. Die funksie is gedefinieer om die totale volume, vrystellingsvolume en hoogte van die dam as die voorspellerveranderlike Hf op te neem. Die doel was om 'n model te ontwikkel wat meer akkuraat as die bestaande modelle is. Die model het relatief goed gepresteer in vergelyking met die bestaande modelle van Rico et al (2008) en Concha Larrauri & Lall (2019), met 'n R^2-waarde van 0,81 en 'n RMSE van 47,72 km. Die hoë wgk-afwyking word toegeskryf aan die variansie tussen die waardes vir D_{max} en Hf. Daarbenewens wissel D_{max} aansienlik tussen ineenstortings en is dit afhanklik van verskillende eksterne faktore soos die topografie van die terrein, of die uitskotstoorgerief naby 'n waterloop is en moontlike natuurlike of mensgemaakte hindernisse.

Model D_{max}.2: Die tweede model wat vir die beraming van D_{max} gedefinieer is, is gemodelleer met behulp van dieselfde 7 gevalle wat vir model V_F.2 gebruik is. Benewens die poelverhouding is die gradiënt van die vloeilyn as 'n veranderlike ingereken. Die helling is vanaf die middel van die uitskotstoorgerief geneem tot by die laagste punt van die vloeilyn van die uitskotmateriaal vanaf die breuk. Die model het relatief goed gepresteer en 'n R^2-waarde van 0,77 en 'n wgk-afwyking van 3 km behaal. Die model is egter baie beperk, weereens vanweë die klein datastel wat beskikbaar was vir ontleding.

Oor die algemeen het die modelle na verwagting gepresteer. Model V_F.1 het die beste gevaar en kan moontlik aangewend word as 'n eerste benadering om die potensiële gevolge van 'n oorstroming na die ineenstorting van 'n uitskotstoorgerief te voorspel, weens die stabiliteit en akkuraatheid wat deur die gebruik van 'n groter datastel teweeggebring is. Die modelle wat ontwikkel is om data van poelverhoudings te bevat, het goed gevaar, maar die datastel moet uitgebrei word om 'n akkurater voorspelling te gee. Hulle toon egter 'n sterk verband tussen die grootte van die oppervlakpoel en die verwagte vrystellingsvolume. Wanneer die modelle oorweeg word wat die afloopafstand voorspel, is dit belangrik om te let op die kompleksiteit van die veranderlikes wat die afvloeiafstand van die uitskot mag beïnvloed. Ondersoeke en modellering van die spesifieke terreine moet gedoen word om die waarskynlikste vloei te identifiseer met inagneming van die aanwesigheid en volume van plantegroei, natuurlike hindernisse en geboue.

Trefwoorde: Uitskot; Ineenstorting; Breekvolume

Table of Contents

List of Figures

List of Tables

1 Introduction

Catastrophic failures of Tailings Storage Facilities (TSF) continue to occur, despite the mining industry making great strides in ensuring that best management practices and safe storage methods are applied. Failures such as Mount Polley (2015), Samarco (2015) and Córrego do Feijão (2019) have shown that malpractice still occurs. All three failures resulted in large volumes of tailings being released which wreaked havoc downstream. Current trends in recorded failure data suggests a decrease in the frequency of failures but show an alarming increase in the magnitude of recorded failures with devastating downstream implications. 49% of all serious and very serious recorded failures since 1940, occurred between 1990 and 2010 (Bowker and Chambers, 2015). This increase in the severity of recorded failures has prompted the mining industry to review existing management practices to ensure an effective loss prevention strategy is followed that would reduce the long-term rate of TSF failures.

Dam breach inundation studies are completed for TSFs as part of the life-of-mine reporting requirements. These studies are normally completed according to national or international guidelines such as those developed by the Canadian Dam Association (CDA) or the International Committee on Large Dams (ICOLD), respectively. A major limitation of these studies is that they do not consider the complex nature of TSF failures as they were developed for clear water flows (Kheirkhah Gildeh *et al.*, 2020). Current software cannot physically model the complex process associated with a TSF failures. Thus, simplified methods such as flowability approximation, geometric estimation and/or statistical regression is used to estimate the volume of tailings released during a hypothetical TSF failure. The statistical regressions were developed using limited datapoints and do not always consider important variables, however, they provide a first approximation of the potential hazard and risk associated with a TSF failure.

1.1 Research Aim and Objectives

The aim of the thesis was to examine the relationship between TSF geometric data and recorded failure data. This will be done to develop an empirical correlation for estimation of potential release volume and run-out distance based on historic tailing dam failures by incorporating the work done by Rico et al (2008), Concha & Lall (2018) and Quelopana (2019) with the work done by Rourke and Luppnow (2015). Each author considered different variables in relation to the volume of tailings released and run-out distance predicted. The empirical correlation for release volume prediction was to be a function of impoundment volume, height, pool ratio prior to failure and for the run-out distance a function of the dam predictor value, the gradient of the flood flow path and the pool ratio prior to failure.

The creation of the database consisted of compiling cases from various literature sources which provided all the required information regarding the failure, including identifying information such as mine name and location. The information required will be the total storage volume of the impoundment, the height of the impoundment, the volume of released material and the run-out distance recorded of

the released material. Without these variables it would not have been possible to derive an accurate and reliable empirical correlation. Additional information that would greatly improve the quality of analysis performed will be type of dam, cause of failure, meteorological events, topography, and volume of ponded water.

The statistical analysis that will be performed will look at the frequency of failures, the types of dams involved in failures and the root causes of failure. A statistical analysis of current industry practices for breach volume and run-out distance estimations will also be conducted to identify possible shortfalls and/or valuable correlations.

1.2 Limitations of Research

The main limitation encountered during the completion of the thesis was the lack of comprehensive TSF failure data. Many of the cases found in literature sources had incomplete information fields. This is attributed to the fact that not all recorded TSF failures are well documented for scientific use and may be purposefully withheld for legal reasons. Due to the misrepresentation of some failure cases, the recorded failure cases were subject to a list of exclusion criteria to ensure the database was as comprehensive as possible. The exclusion criteria were:

- Failure cases where any quantitative data was missing, such as the total storage volume (V_T), recorded release volume (V_F) and dam height (h), was omitted from the final database.
- Failure cases that did not have the recorded run-out distance (D_{max}) values were omitted from the correlation analysis for $D_{P.max}$.
- Only cases that qualify as failures according to International Committee On Large Dams (ICOLD) classifications, shown in Table 3-1, would be used for the analysis

Additional limitations were encountered when assessing the effect of the pool ratio on the magnitude of failure. In order to estimate the pool ratio prior to failure, Google Earth imagery was used to calculate the surface area of the TSF and the surface area of the ponded water. The major limitation was the availability of imagery that presented well-defined images of the TSF in the year of failure. This was due to weather events affecting the visibility of the TSF and failures that occurred prior to 2000 did not present images with the necessary resolution to be used for these calculations.

1.3 Thesis Layout

This thesis consists of seven chapters. The first chapter is a basic overview of the project with a short background on Tailings Dam Breach Assessments (TDBAs), the motivation, objectives, and limitations of the research. It also provides a short overview of the study areas of the research with brief descriptions of each. Chapter 2 provides a literature review of tailings storage facilities, their construction methods, trends in failure data and mechanisms of failure. Further it examines the current industry practices and

empirical relationships that are used during inundation studies. The chapter also briefly discusses the modelling software used during the regression analysis phase of this thesis.

Chapter 3 describes the methods employed to construct the failure database, highlighting the specific selection criteria for cases to be added, describes the methods used for gathering site specific data such as pool ratio prior to failure and the gradient of the tailings flood flow path. The chapter further defines the four models that was developed for the estimation of potential release volume (V_F) and run-out distance (D_{max}).

Chapter 4 presents the results and discussion of the empirical correlation analysis done using Eureqa and compares the accuracy of the developed models to existing models when applied to the updated failure database. Chapter 5 is a short conclusion chapter with recommendations for further research. Chapter 6 lists all the references used whilst completing this thesis and the appendices are contained in Chapter 7.

2 Literature Review

This chapter presents the literature that has been reviewed, in order to firstly ensure a firm understanding of mine waste material and their disposal practices, secondly to identify and understand the various failure mechanisms leading to TSF failures. Further the chapter examines the various empirical methods used during Breach Volume prediction studies.

2.1 Mine Waste Material

Mine waste material broadly refers to any material which is found to not contain valuable ore minerals or is below the cut-off grade of the mine. The cut-off grade of the mine is determined by the market value of the ore contained in each mined unit of rock compared to the cost of mining said unit of rock (Hitch, Ballantyne and Hindle, 2010). Waste material is continuously generated throughout the life cycle of a mine as by-products of various operations, with the type of waste varying with the operation being performed (Harraz, 2010). The three main types of waste are mine waste rock, mine waste water and tailings material, Figure 2-1 summarises the main sources of waste materials (Geological Survey of Sweden, 2019).

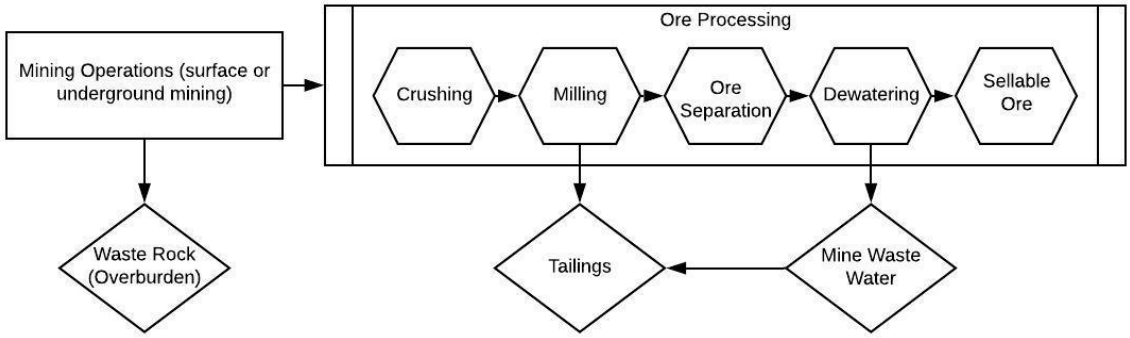

Figure 2-1: Simplified Mine Waste origin diagram indicating the three main waste streams, adapted from Bian, Miao, Lei, Chen, Wang & Struthers, (2012).

Waste rock is produced during the excavation phase of mining and ranges in size from large boulders to sand-size particles, depending on the nature of the overburden and host ore body. It is the overburden rock that needs to be removed in order to reach the ore body, this might include ore that is below the cut-off grade of the deposit (Hitch, Ballantyne and Hindle, 2010). As global ore grades diminish, the average stripping ratio of mines increases which in turn increases the amount of waste rock produced (Das and Choudhury, 2013). Waste rock is commonly discarded of on waste piles that are located close to the mine pit where it is easily accessible by road. Waste rock may be classified as Non-Acid Generating rock (NAG) or Potential Acid Generating rock (PAG). PAG waste rock commonly contain sulphide minerals which are easily weathered when in contact with oxygen and may produce acid water leading to Acid Mine Drainage (AMD) and the leaching of toxic, heavy metals that contaminate the

natural water body (Lefebvre, 1995). In some situations, it is necessary to line these waste rock piles with a geosynthetic membrane to prevent contamination of natural water resources.

However, when waste rock is found to have the desired strength and geotechnical characteristics it may be repurposed as construction materials ranging from aggregate, used in civil construction, to materials used to construct mining infrastructure such as TSF. During the closure period of mines, waste rock is commonly used as a backfill material to ensure the stability of pit walls and provide favourable conditions for vegetation regrowth.

Mine waste water does not have a single source but instead originates continuously from multiple operations conducted at a mine (Mohapatra and Kirpalani, 2017). Waste water originating from the processing plant and as surface run-off pose significant risks to natural water resources and local communities as they are not suitable for consumption or domestic use (Dharmappa, Sivakumar and Singh, 1995; Geological Survey of Sweden, 2019). Mine waste water is stored and/or treated to ensure minimum quality standards are met before being released into natural water sources, these treatments can be done using a treatment facility or by storing the waste water in a containment facility to allow natural physical and biological processes to remove/reduce the levels of contaminants present (Kalin, 2004).

Tailings waste material is defined as the fine grained material, sand to silt sized, generated during the recovery of mineral commodities and is generally in the form of slurry (UNEP and Mining Journal Research Services, 1996). Depending on the host geology, the tailings slurry may contain hazardous materials such as cyanide, arsenic, sulphidic compounds etc. that are associated with leaching and other beneficiation processes required to liberate the target mineral (UNEP and Mining Journal Research Services, 1996; Das and Choudhury, 2013). Tailings material is stored using various methods depending on a multitude of factors such as economic feasibility, geographic location, volume of tailings expected to be produced, climatic conditions and environmental impact (Australian Government Department of Industry Tourism and Resources, 2016). Examples of different methods of storage include backfill practices, thickened paste, dry stacking and surface TSF, the latter being more common (Dold, 2014; Harraz, 2010). These methods will each be discussed in the next section.

2.2 Tailings Disposal Methods

Historically tailings material has been disposed of in the most cost effective and convenient manner, without much regard for environmental impact or safety performance (U.S Environmental Protection Agency, 1994). Only after concerns regarding the downstream environmental and socio-economic effects of uncontrolled tailings disposal were raised did the mining industry move towards current conventional storage techniques.

Safely disposing of mine waste material is one of the largest challenges faced by the mining industry worldwide, with mining houses incurring major expenses to ensure responsible practices are employed (Coumans, 2002). Dealing with the colossal amounts of mine waste generated each year requires innovative design and planning to ensure this challenge is met. The selection of the appropriate disposal method is dependant of various operational and environmental factors that are unique to each project, summarised in Table 2-1. The continuum of tailings material described in Figure 2-2 illustrates the main difference between the different states that tailings material is stored.

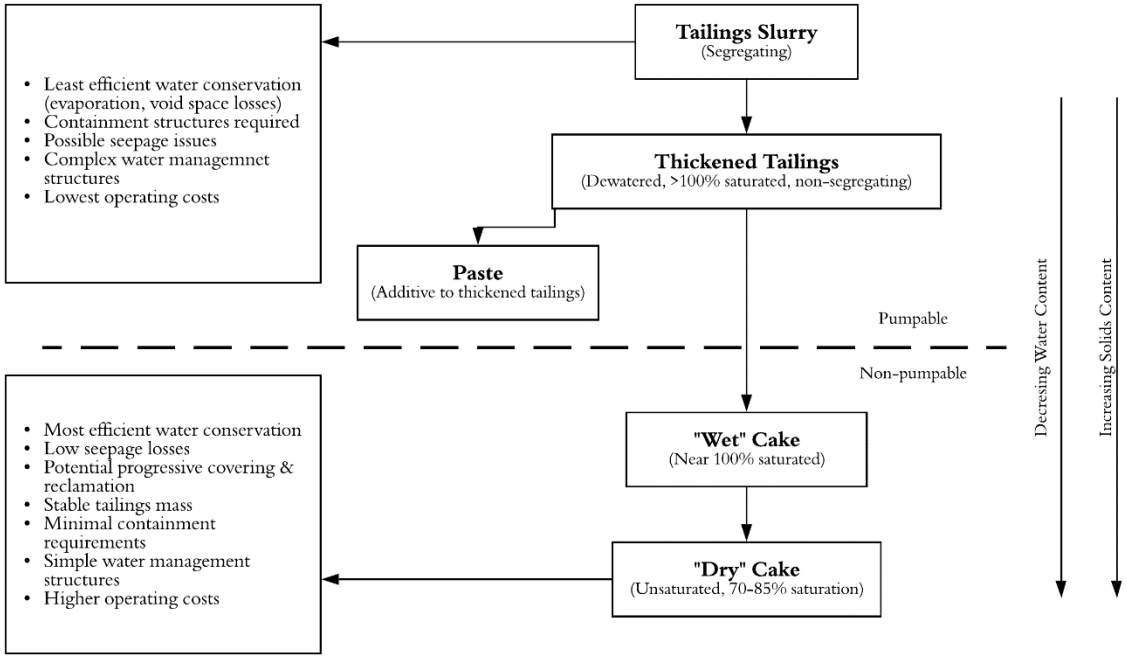

Figure 2-2: Diagram depicting the tailings continuum as described by Davies (2011).

The tailings continuum as described by Davies (2011) illustrates the different methods of waste disposal based on the tailings physical characteristics, specifically the water content and its ability to be pumped to a storage facility. An important factor to consider is that a decrease in the water content of the tailing material relates to an increase in transportation cost to the storage facility. However, when the water content of the tailings is decreased, the tailings material becomes more suitable for use in self-supporting structures such as stacks. The method employed for disposal is therefore dependant on site specific requirements.

Table 2-1: Factors influencing selection of tailings disposal method (after Australian Government Department of Industry Tourism and Resources, 2016) .

Operational	Environment
Extent of pre-disposal dewatering dependant on: • Rheology and transportability of tailings • Chemical and biological reactivity of tailings • Return water requirements • Process water quality and suitability for re-use • Availability of raw water	• Climatic conditions • Site topography • Distance and elevation of selected TSF • Regulator imposed conditions

The most common method used to store tailings material is in surface retaining structures that have been constructed for this specific purpose. The tailings slurry is transported from the ore processing facility via pipeline to the designated TSF where it is hydraulically deposited. As the slurry accumulates, gravity induced segregation ensures that coarser particles are deposited closer to the discharge point and finer particles are carried away (Klohn Crippen Berger, 2017). Due to the high-water content of the slurry material, excess water will accumulate and form what is called a supernatant pond. The supernatant water and surface run-off water may be recycled by means of a decant systems present around the perimeter (Australian Government Department of Industry Tourism and Resources, 2016).

Paste or thickened tailings refers to tailings that have been extensively dewatered during pre-disposal processes through mechanical means or by adding industrial thickening agents, thickened to >60% pulp density and <25% moisture content (Australian Government Department of Industry Tourism and Resources, 2016; U.S Environmental Protection Agency, 1994). Through these processes, excess water is recycled and the solid to water ratio increases. Industry trends indicate more mines are leaning toward dewatering processes as seen in Figure 2-3. By applying dewatering processes to tailings material pre-disposal, the amount of ponded water will be reduced and, in some cases, eliminated which in turn reduces the risk of catastrophic failures and downstream devastation (Li *et al.*, 2009; Klohn Crippen Berger, 2017).

Co-disposal of coarse mine waste rock and tailings, commonly disposed of in an open pit, has the benefit of reducing the volume or footprint required for storage as the fine-grained tailings fill the voids left by the waste rock whilst providing a more stable deposit (Australian Government Department of Industry Tourism and Resources, 2016). Co-disposal techniques have a relatively low permeability making it ideal for storage of PAG wastes as the higher moisture content acts as an oxygen seal prohibiting acid generation (Cunning and Hawley, 2017).

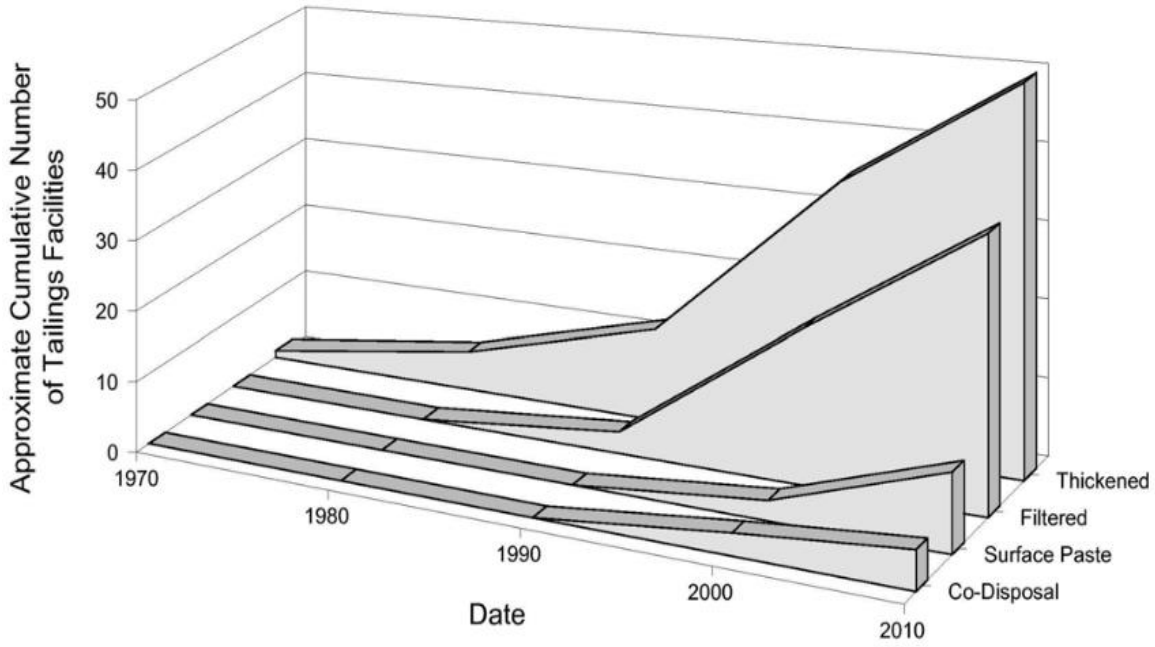

Figure 2-3: Global trends in use of Dewatered Tailings methods in mining after Davies (2011).

2.3 Raised Embankment Structures

Raised embankments are commonly constructed using readily available material such as waste rock, natural soil or tailings and is systematically raised at height intervals as more storage volume is required (Vick, 1990). This has the benefit of lowering initial capital costs for the project, instead phasing placement and fill material costs over the life of the impoundment (U.S Environmental Protection Agency, 1994). Three main construction types exist, upstream, downstream and centreline, referring to the direction the embankment crest moves (Sarsby, 2000). These construction types can be applied in various topographical environments through the construction of valley impoundments, and configurations thereof, and as ring-dike structures on flatter terrain (U.S Environmental Protection Agency, 1994).

2.3.1 Upstream

The upstream construction method has the lowest initial capital requirement of the three methods due to the minimal amount of fill material required for starter dike construction and subsequent raises (Vick, 1990). The construction sequence is illustrated in Figure 2-4. Construction commences with a starter dike composed of either waste rock, natural soil or coarse tailings that are compacted to provide a stable footing after which tailings material is discharged into the impoundment (Holmqvist and Gunnteg, 2014). As the impoundment fills subsequent dikes are constructed on the coarse tailings by placing natural soil or raking the coarse tailings to form the next dike. It is important that the tailings beneath the newly constructed dike form a competent foundation to support the construction of subsequent dikes, in some cases requiring some form of mechanical compaction (U.S Environmental Protection Agency, 1994). Vick (1990) states that due to the tailings material having to support the load of the dike, the tailing material should contain no less than 40 to 60 % sand, this eliminates the upstream

method from being implemented at operations with very fine grained mill tailings (U.S Environmental Protection Agency, 1994; Holmqvist and Gunnteg, 2014).

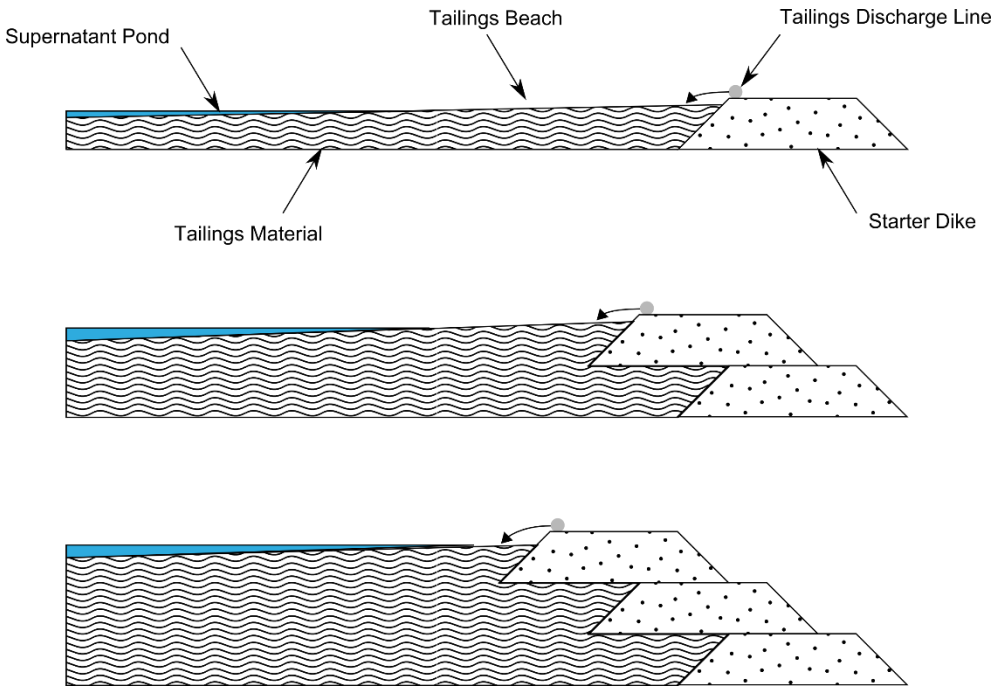

Figure 2-4: Upstream dam construction sequence after Vick (1990).

The application of upstream construction methods is limited by its poor seismic performance, sensitivity to phreatic level migration, water storage capacity and rate of dam raising (Vick, 1990; U.S Environmental Protection Agency, 1994). Upstream type constructed embankment dams are sensitive to seismic induced liquefaction due to their low relative density and high saturation levels. Vick (1990) describes three variables that control the phreatic surface location described in Figure 2-5 below.

Figure 2-5 (a) illustrates that a high pond level may lead to the phreatic surface encroaching on the embankment face which may lead to slope instability. A high pond level may also lead to overtopping and subsequent erosion on the embankment face. Therefore, upstream type dams require constant and careful monitoring of the supernatant pond to ensure it stays within operational limits. Figure 2-5 (b) illustrates the effects of beach segregation on the position of the phreatic surface relative to the embankment face, a higher beach gradation allows for a stronger, more permeable crest to form which promotes better water drainage through the embankment. Figure 2-5 (c) illustrates the importance of having adequate foundation drainage in place to ensure the phreatic surface does not rise. The rise rate of upstream embankments is limited since excess pore water pressure may develop if the drainage rate

is not adequate (Holmqvist and Gunnteg, 2014). This decreases the stability of the foundation layers and may lead to failure.

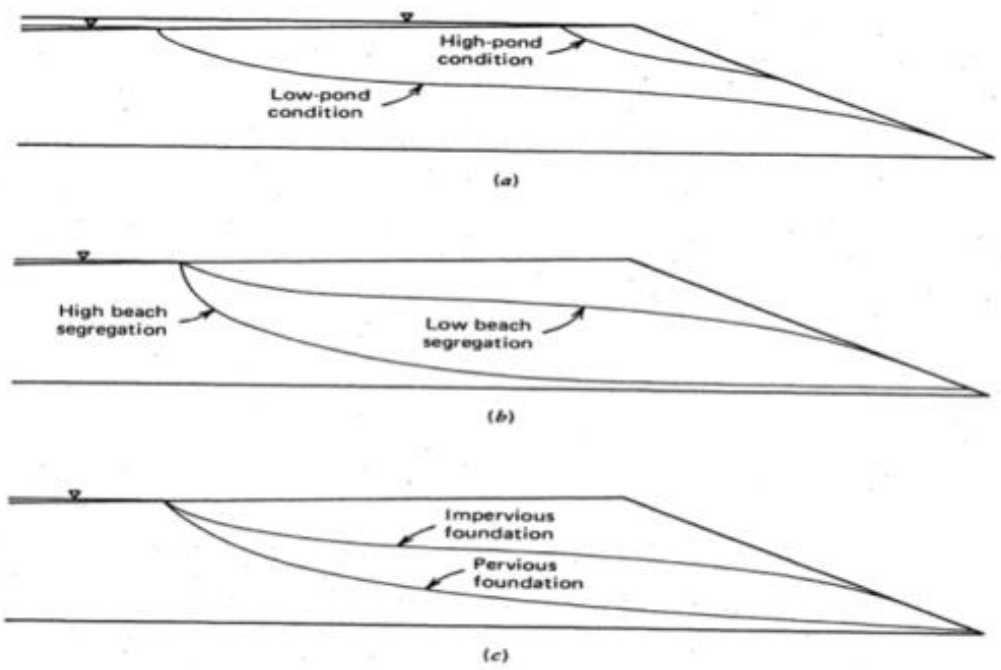

Figure 2-5: Effects of various controls on the phreatic surface. (a) Pond water level. (b) Beach grain size segregation and lateral permeability variation. (c) Foundation permeability from Vick (1990).

2.3.2 Downstream

The downstream construction method commences with a similar starter dike as the upstream method being filled with slurry material, subsequent raises are then constructed on the downstream slope of the starter dike with the downstream slope being roughly equal to the angle of repose of the material used, as shown in Figure 2-6. The design requirements are similar to those of a water retention dam, hence the downstream method can accommodate larger amount of water without having to take the phreatic surface into consideration (U.S Environmental Protection Agency, 1994).

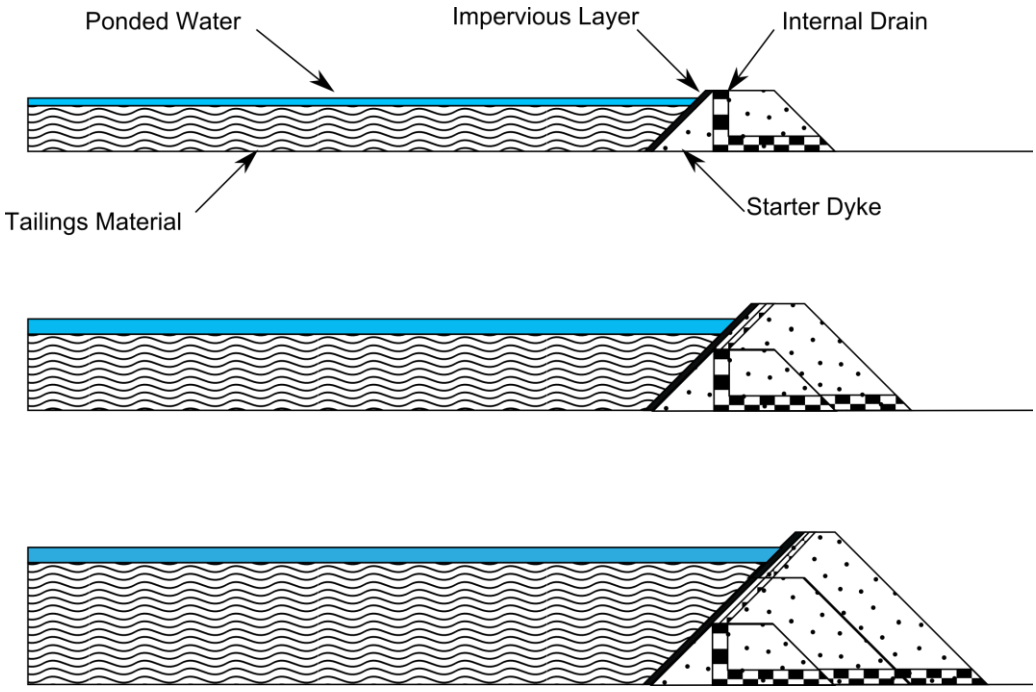

Figure 2-6: Downstream dam construction sequence adapted from Vick (1990).

The advantages of employing the downstream raising method is the ability to install internal drains and impervious layers to control the phreatic surface, and that the raising rate of the dam does not affect the phreatic surface level (Holmqvist and Gunnteg, 2014). The downstream construction method is also more resistant to seismic action. Tailings material is pumped into the impoundment through peripheral spigots or a central cyclone after which the coarse tailings is raked outward and compacted (U.S Environmental Protection Agency, 1994). The downstream raising method requires careful planning to ensure the embankment toe has enough downstream freeboard to progress as the height increases, this is normally the controlling factor on the height of the dam (Vick, 1990). A major disadvantage of this method is the large volume of embankment material required for construction, making this method comparatively costlier than the upstream method.

2.3.3 Centreline

The centreline raising method is seen as a compromise between the two methods mentioned above, combining their advantages, and mitigating their disadvantages. The centreline method requires less material than the downstream method and is more resistant to seismic events than the upstream method. Internal drainage systems help to control the phreatic surface of the tailings deposit (Vick, 1990). Figure 2-7 depicts the sequence of construction for a centreline embankment dam. The centreline method can accommodate large amounts of water from heavy precipitation events for a short term whilst still maintaining its stability (U.S Environmental Protection Agency, 1994)

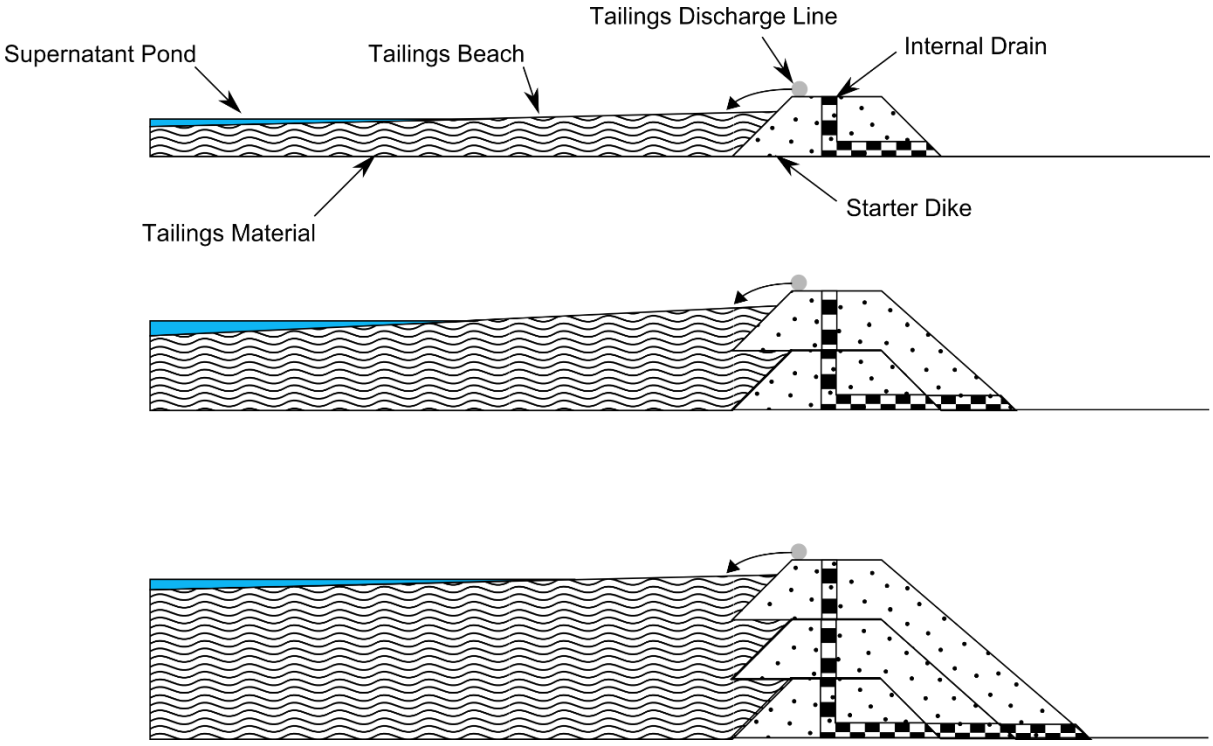

Figure 2-7: Centreline construction sequence (Vick, 1990).

2.4 Catastrophic TSF Failures

Catastrophic failures of a TSF can have devastating effects on the surrounding communities, environments, and mining companies. Less severe failures such as cases of uncontrolled seepage can also adversely affect the environment, specifically sensitive water sources (ICOLD, 2001). A TSF failure can be described as the inability of the storage structure to meet its design intent and which may result in the uncontrolled release of mobilised tailings, resulting in a loss to stakeholders and the environment (Martin, Al-Mamun and Small, 2019). It is imperative that we review and learn from past incidents of failure to ensure future risk of failures be mitigated. However, to ensure reliable data on TSF failures is available for review, there must be unbiased reporting of failures by countries. Martin *et al.* (2002) notes that the reporting of failures is often incomplete and biased with no worldwide database that documents failures. Many TSF failures are simply not reported due to fear of legal implications and impact on public opinion (Kossoff *et al*, 2014). Since then an attempt has been made by Bowker *et al*. (2019) to compile a global database of recorded failures since 1915.

The catastrophic failure at the Córrego do Feijão TSF in 2019 prompted the International Council on Mining and Metals (ICMM), the United Nations Environment Programme (UNEP) and the Principles for Responsible Investment (PRI), to conduct a global tailings review and ensure that global best practices are employed (International Council on Mining & Metals, 2020). As part of this review, 726 extractive companies were contacted to complete a questionnaire regarding their management of tailings storage facilities. Using information gained from interactions between investors and extractive

companies, the ICMM, UNEP and PRI were able to release a Global Industry Standard on Tailings Management which aims to mitigate failure risk of TSFs by implementing industry best practices.

2.4.1 Failure Trends

There are an estimated 3500 TSFs globally, both active and inactive, with active facilities being more likely to fail (Kossoff *et al.* 2014; Rico *et al*. 2008). The rate of failure for these TSFs has been estimated to be between 2 and 5 per annum (Davies, Martin and Lighthall, 2000). What has become apparent from recorded failure data is that although the frequency of failures is decreasing, the amount of serious and very serious failures has been increasing in the last two decades, with 49% of all recorded serious and very serious failures having occurred since 1990 (Bowker and Chambers, 2015). Figure 2-8 illustrates the decrease in failures per decade but shows an upward trend of high-consequence failures since 1980.

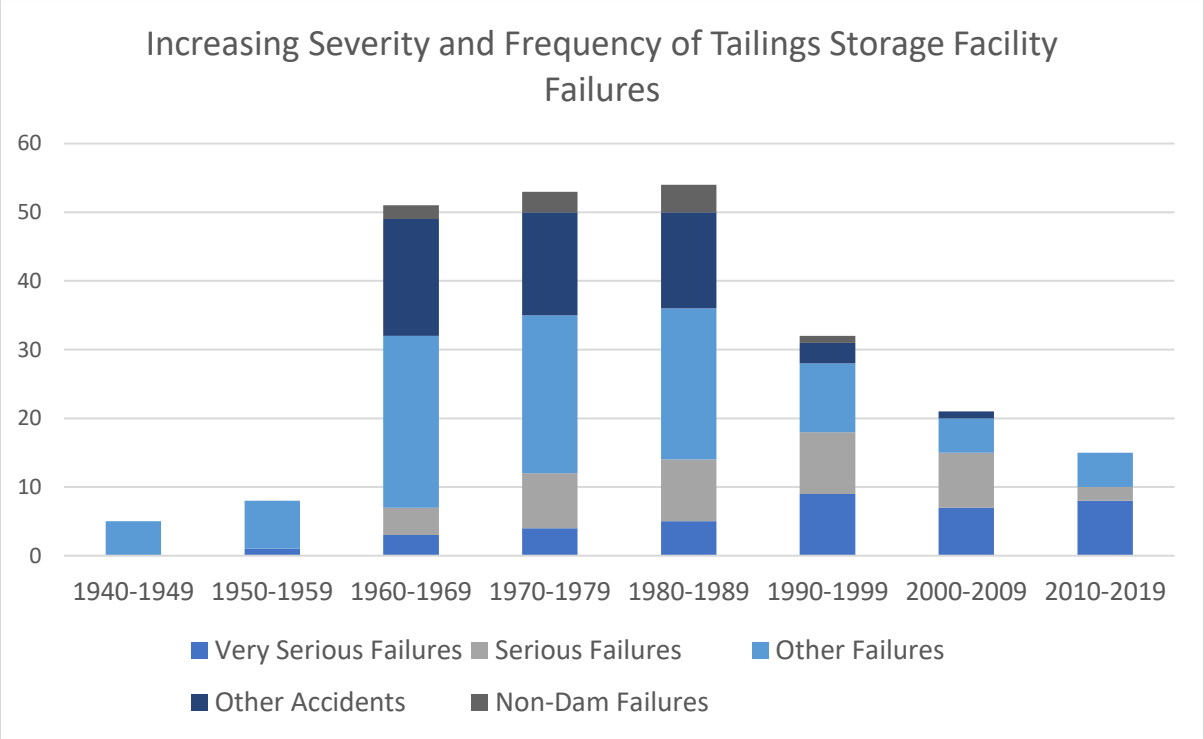

Figure 2-8: Frequency of failures based on severity rating from Bowker & Chambers, 2017 *(Very Serious > 1Mm^3 released, Serious >100 000 m^3 released).*

Some of the most severe failures occurred in the last decade, failures such as the Ajka Alumina in Romania (2010), Philex Padcal in the Phillipines (2012), Mt Polley in Canada (2014), Samarco in Brazil (2015), Cadia mine in Australia (2018) and San Brumadinho in Brazil (2019) (Bowker *et al.*, 2019; Owen *et al.*, 2020; Rico *et al.*, 2008).

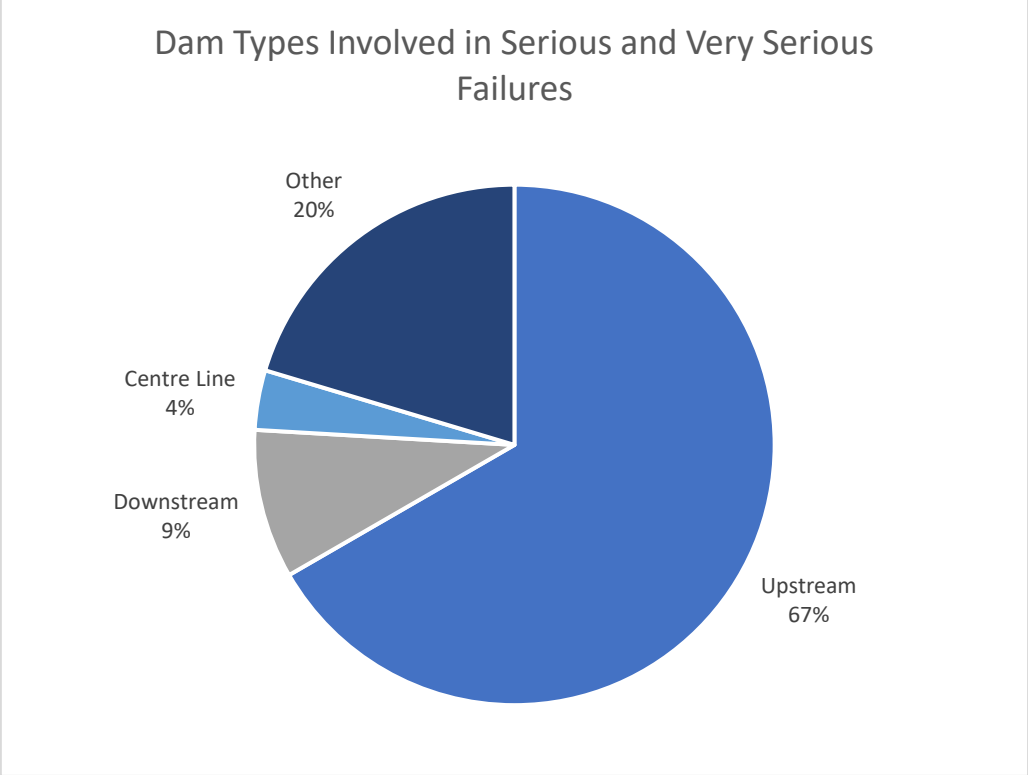

Figure 2-9: Failures of main dam types from Bowker *et al.* (2019)

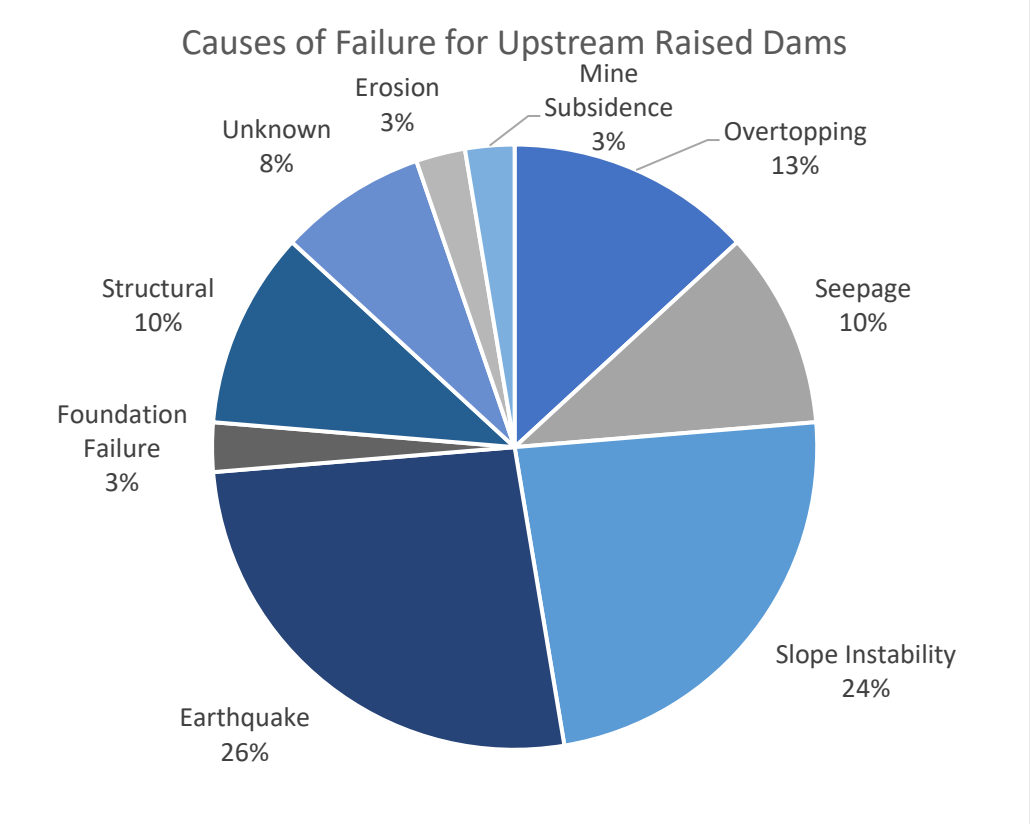

Figure 2-10: Causes of failure associated with upstream raised dams, from Bowker *et al.* (2019).

2.4.2 Failure Mechanisms

Failures may be attributed to a singular or a combination of different failure modes. The main failure modes identified by Engels (2004), Roca, Murphy & Vallesi (2019), Roche, Thygesen & Baker (2017) and U.S Environmental Protection Agency (1994), include overtopping, erosion (internal and external), foundation failure, earthquake damage and structural failure. Table 2-2 summarises credible defects associated with TSFs as described by Engels (2004). The author noted that the majority of the defects are detectable through regular inspection and monitoring.

Table 2-2: Summary of credible defects commonly associated with TSFs, with causes and methods for detection from Engels (2004).

Type of Defect	Cause	Possibility of detection by inspection and/or monitoring
Overtopping	Inadequate hydrological or hydraulic design	Regular inspection may reveal problem
	Loss of freeboard due to crest settlement	Detectable by survey and inspection
Slope Instability	Overstressing of foundation soil and dam fill	Line and level survey, inclinometer monitoring and inspection may reveal potential problem
	Inadequate control of water pressure (pore pressure)	May be detectable by piezometer and seepage monitoring
Internal Erosion by Seepage	Inadequate control of seepage	May be detectable by piezometer and seepage monitoring, difficult to detect in early stages but seepage flow monitoring may reveal potential problem
	Bad filter and drain design	
	Poor design or construction control resulting in cracking	
External Erosion	Inadequate slope and toe protection	Detectable by inspection
Earthquake Damage	Inadequate geometry (slope too steep)	Inspectable post non-catastrophic event may highlight design shortcomings
	Liquefaction of tailings, embankment, or foundation soils	Piezometer monitoring post non-catastrophic event may indicate potential of liquefaction
Groundwater Pollution	Seepage of leachate into groundwater, due to lack of or deterioration of liners	Detectable by monitoring of observation wells
Damage to Decant Systems	Excessive settlement	Possibly detectable by inspection
	Chemical attach on cement/steel (oxidation etc.)	

Foundation failure occurs when the underlying geology is incapable of supporting the load of the embankment and TSF, this may lead to movement on the failure plane which allows the formation of seepage paths and differential settlement of the embankment and/or tailings material (Roca, Murphy and Vallesi, 2019).

Overtopping is one of the most common causes of failure in TSFs, and is defined as when the free water, or supernatant pond, on an impoundment rises above the crest of the embankment and flows over the downstream face (U.S Environmental Protection Agency, 1994). Overtopping can be the result of poor design, crest erosion, crest subsidence, poor management or heavy rainfall events (Roca, Murphy and Vallesi, 2019). Roca *et al*. (2019) noted that overtopping accounted for 80% of inactive dam failures which highlights the importance of continuous monitoring and management even after closure. Overtopping may lead to the erosion of the embankment dam due to the erodible nature of the fill material used for construction and a rapid increase in pore water pressure which may result in the liquefaction of the unconsolidated waste material.

Erosion of the embankment face or abutments occur when inadequate storm water diversion measures are employed, and the exposed embankment bears the brunt of the flow. This type of failure is preventable by covering the embankment to protect the exposed fill material (U.S Environmental Protection Agency, 1994). Internal erosion, referred to as seepage or piping, occurs when tailings material is washed through settlement cracks etc. and commonly occurs around conduits (Roca, Murphy and Vallesi, 2019). This has a cascading effect and the problem becomes worse as more fill material is being washed away (Engels, 2004).

Liquefaction, static or dynamic, of tailings material may be earthquake induced under cyclic loading of the tailings sediment, which typically consists of an unconsolidated, uniform graded material. Upon loading the pore water pressure increases. Per Terzaghi's Principle of Effective Stress, when the effective stress is equal to zero, the material will behave as a liquid (Engels, 2004; Pacheco, 2019).

Slope instability failure normally occurs in two forms, rotational or sliding failure, and is due to the shear stresses in the dam exceeding the shear resistance of the dam (Roca, Murphy and Vallesi, 2019). The shear stresses of tailings material are directly proportional to the density and degree of compaction of the tailings, and indirectly proportional to the pore water pressure (i.e. a higher phreatic surface leads to increased pore water pressure and decreased resistance to shear failure) (Engels, 2004).

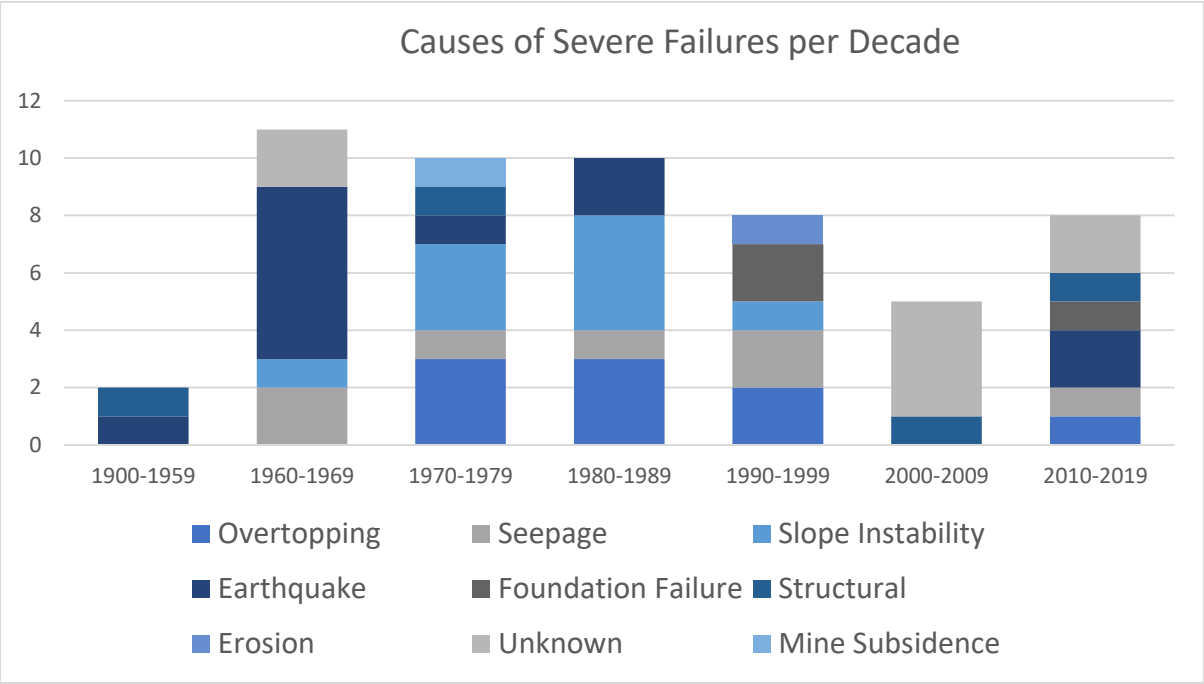

Figure 2-11: Recorded causes of failure over the past 120 years from Bowker *et al.* (2019).

2.5 Current Industry Practices for Inundation Studies

Recent catastrophic failures of TSFs have prompted the mining industry to assess and improve the manner in which tailings dam breach analyses (TDBAs) are conducted. The Canadian Dam Association (CDA) has recently released a technical bulletin on TDBAs which aims to provide industry professionals with guidance regarding the general process and scope of conducting these analyses (Martin, Al-Mamun and Small, 2019). This technical bulletin will expand on the previous bulletins, 2007 CDA Technical Bulletin: Inundation, Consequences and Classification for Dam Safety and on the 2014 CDA Technical Bulletin: Application of Dam Safety Guidelines to Mining Dams. In addition to the technical bulletin, mine owners have started to develop internal guidelines for conducting TDBA. The CDA Bulleting suggests that the characteristics and volume of released tailings is dependent on two factors:

- The presence of fluids on the tailings surface, supernatant or fluid tailings
- The liquefaction potential of the tailings material due to various trigger mechanisms.

These factors are then used to define the TSF as one of four types of TDBA cases that describe the breach event characteristics and aid in estimating the potential outflow volume of fluids and tailings that may be released (Martin, Al-Mamun and Small, 2019), see Table 2-3. See appendix A.1 for a description of the TDBA process flow.

To improve the current models used to assess the hazard and risk posed by TSF, it is necessary to gain a better understanding of TSF breach mechanisms and run-out characteristics (Kheirkhah Gildeh *et al.*, 2020). An integral part of the TDBA process is understanding the relationships between available TSF

failure data and dam geometric characteristics. Increased research into these relationships will lead to improving the accuracy of current TDBAs.

Table 2-3: TSF failure assessment cases for TDBAs according to CDA Technical Bulletin 2020, from Kheirkhah Gildeh *et al.*, (2020).

Presence of supernatant pond?	**Potential for tailings runout as a result of flow liquefaction[1]?**	
	Yes	**No**
Yes	Case 1A: Liquefied tailings with a pond. Dam breach with flow of fluids and eroded, liquefied flowable tailings contributing to additional volume of materials released.	Case 1B: Non-liquefied tailings with a pond. Dam breach with eroded tailings, transported and deposited by the flow of fluids.
No	Case 2A: Liquefied tailings without a pond. Dam breach resulting from slope failure with mudflow of liquefied flowable tailings (dependent of degree of saturation).	Case 2B[2]: Non-liquefied tailings without a pond. Slope failure of the dam.

Part of the TDBA process is to estimate the potential release volume of a hypothetical tailings breach, this is extremely complicated due to the high level of uncertainty associated with such an analysis (Kheirkhah Gildeh *et al.*, 2020). Simplified methods of estimating the potential release volume can be done through statistical regression studies, flowability approximation and geometric characteristics. Up until 2008, dam break analysis was developed for water storage dams specifically, since then there have been various attempts at developing empirical prediction models through statistical regression studies that take the high sediment load and differing dam characteristics into account (Rico *et al.*, 2008). For the purpose of this thesis, four empirical models developed by Rico et al (2008), Rourke & Luppnow (2015), Concha & Lall (2018) and Quelopana (2019) will be assessed and discussed in this section. These models aim to estimate the potential risks and downstream impacts associated with TSF failures, by using the basic dam geometric characteristics of the TSF. The models obtained by the four studies are summarised in Table 2-4.

[1] Flow liquefaction of tailings can be induced by any potential trigger (static or cyclic loading) including shear strains in the tailings as a result of the dam breach.
[2] Hydrological analyses will not be required, instead consider a landslide runout analysis.

Table 2-4: Empirical correlations currently in use (V_F = Volume of material released, V_T= total storage volume, PR= Pool Ratio[3], D_{max}= Outflow volume, H= Height of dam, $H_f = H \times (\frac{V_F}{V_T}) \times V_F$)

	V_F Correlation Equation	**R^2**	**D_{max} Correlation Equation**	**R^2**	**Data points**
(Rico, Benito, Diez-Herrero, *et al.*, 2008)	$V_F = 0.354 \times V_T^{1.008}$	0.86	$D_{max} = 1.612 \times (HV_F)^{0.655}$	0.57	28
(Rourke and Luppnow, 2015)	$V_F = 0.6533 \times PR + 0.0136$	0.99	-		5
(Concha Larrauri and Lall, 2018)	$V_F = 0.332 \times V_T^{0.95}$	0.88	$D_{max} = 3.04 \times H_f^{0.545}$	0.65	29
(Quelopana, 2019)	$V_F = 0.0612 \times V_T^{0.809} \times h^{0.544}$	0.91	-		35

[3] Pool ratio is defined as the ratio between the total surface area of the TSF and the surface area of the supernatant pond.

Rico et al. (2008) set out to develop a set of basic empirical relationships that aim to provide a first and universal way to measure potential risk and impact of TSF breaks based on basic physical characteristics of historic failures. Hagen (1982) and Petrascheck (1984) identified that the reservoir volume and dam height are critical factors in the magnitude of failure for dam breaks. Rico et al (2008) noted that for TSF, the release volume is dependent on factors such as breach size, the extent of material liquefaction and the size of the supernatant pond at the time of failure. Given that the freeboard of a TSF is relatively small, the height of the dam crest was defined to be a good approximation of the thickness of the tailings bed and hence the potential energy during a TSF failure.

When developing the model for the prediction of the run-out distance (D_{max}), Rico et al (2008) found a weak relationship between the dam height (h) and the recorded run-out distance shown in Figure 2-12. A slightly better relationship was found when assessing the recorded outflow volume against the recorded run-out distance, shown in Figure 2-13. The authors did not find a significantly better relationship when considering the relationship between the dam factor (H x V_F) and the recorded run-out distance, shown in Figure 2-14. Rico et al (2008) suggested that these poor correlations found are due to the model not accounting for the presence of high viscosity tailings, possible obstacles that prohibit extensive outflow, TSF with low slope gradients, local topography and associated adverse meteorological events prior to failure. When developing the model for the prediction of potential release volume, Rico et al (2008) found a strong relationship between the impoundment volume (V_T) and the recorded release volume, shown in Figure 2-15. The relationship shows that on average a third of the impoundment volume will be released upon failure, this includes tailings and water in the decant pond.

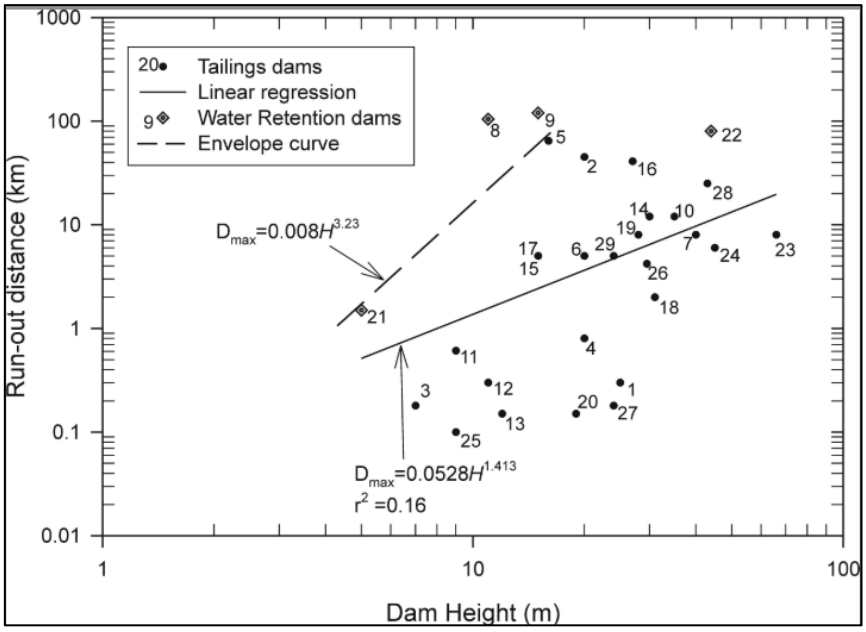

Figure 2-12: Relationship observed between the recorded run-out distance and the dam height at the time of failure, from Rico *et al.* (2008).

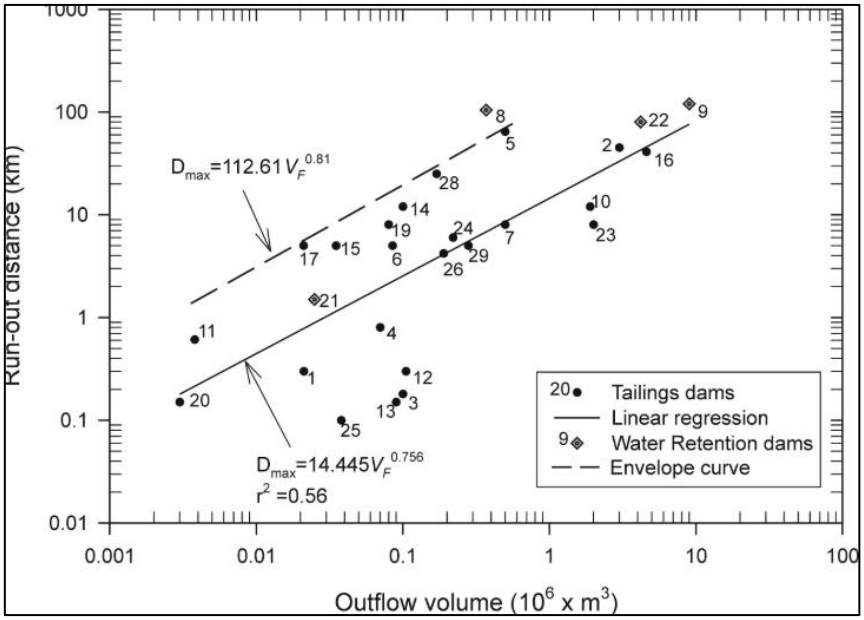

Figure 2-13: The relationship observed between the recorded run-out distance and the recorded outflow volume, from Rico *et al.* (2008).

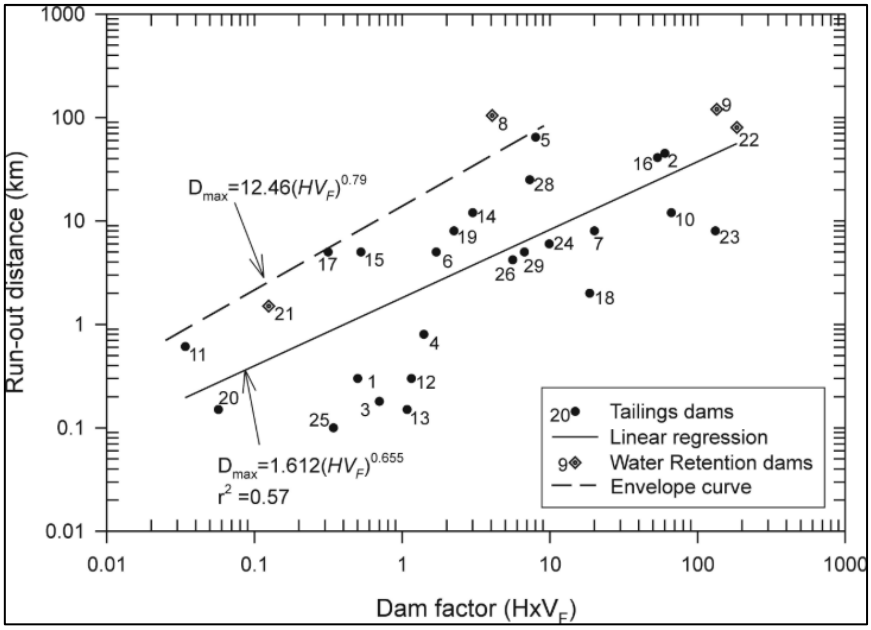

Figure 2-14: The relationship observed between the recorded run-out distance and the dam factor, from Rico *et al.*, (2008).

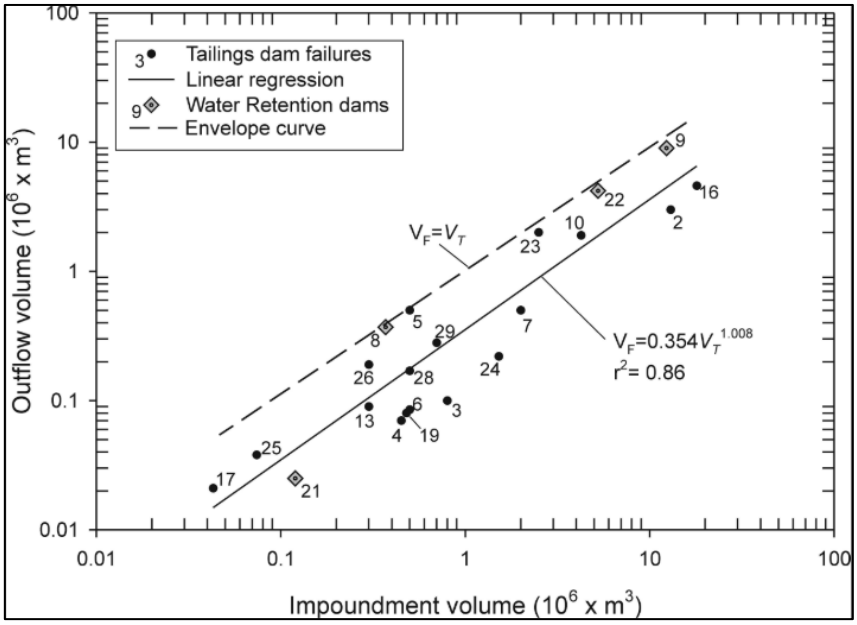

Figure 2-15: The relationship observed between the recorded release volume and impoundment volume, from Rico *et al.* (2008).

Concha Larrauri & Lall (2018) set out to develop an updated statistical model of the empirical correlations developed by Rico et al. (2008). The authors compared the results obtained by Rico et al. (2008) with the results achieved using an updated dataset which includes new cases from the WMTF database compiled by Chambers and Bowker (2019). The authors proposed the introduction of a new predictor (H_f) which they hypothesized would provide a better estimation of run-out distance. H_f is defined in Eq. 1:

$$H_f = H \times (\frac{V_F}{V_T}) \times V_F \qquad \text{Eq. 1}$$

Concha Larrauri & Lall (2018) observed a strong relationship between the impoundment volume (V_T) and recorded release volume (V_F), as shown in Figure 2-16 (1), when testing on the updated dataset. The authors observed a poor relationship with large dispersion between the dam factor (H x V_F) and recorded run-out distance, shown in Figure 2-16 (2). The relationship between the predictor H_F and recorded run-out distance was not found to be significantly better than previous attempts, but the points did present a smaller observed dispersion, see Figure 2-16 (3). Concha Larrauri & Lall (2018) noted that when using more datapoints in the regression for the estimation of release volume, the uncertainty of prediction for larger failures decreases. The authors found that the model developed for the prediction of run-out distance using the predictor H_F was an improvement on the model developed by Rico et al. (2008), as it considers the potential energy of the released volume of tailings as opposed to the total volume of the impoundment.

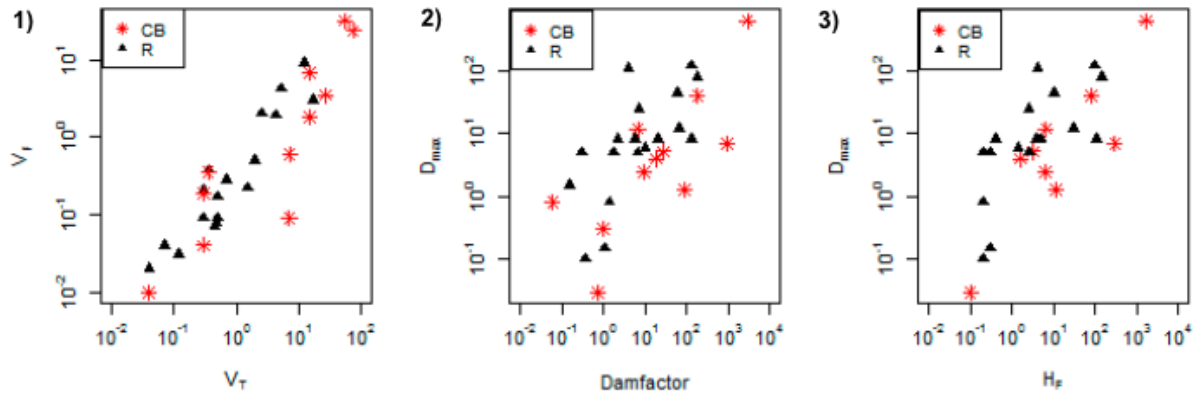

Figure 2-16: The relationships observed between:1) Impoundment volume (V_T) and Release volume (V_F), 2) Recorded run-out distance (D_{max}) and the dam factor, 3) Recorded run-out distance (D_{max}) and the predictor Hf.

Quelopana (2019) set out to improve on the existing empirical relationships for the prediction of release volume (V_F) defined by Rico et al. (2008) and Concha & Lall (2018), by incorporating the dam height (h) in the model. The author made the following changes to the existing databases:

- Cases where V_F and V_T values were missing, V_T values did not match the dam dimensions and where the released volume corresponds with water, were removed.
- Values of some cases were updated by subtracting the volume of water, if known, from the total volume and release volume.
- 12 new cases were added which were not included in previous databases.

The author made the following assumptions when developing the empirical relationship:

1. That the release volume is a function of the tailings storage volume and the dam height.
2. That the influence of each key parameter can be evaluated in a separated way through power functions.

Quelopana (2019) found a poor correlation between the dam height and the recorded release volume, shown in Figure 2-17. A strong relationship was found between the impoundment volume and the recorded release volume, shown in Figure 2-18. When testing the model developed by the Quelopana (2019) against the existing models developed by Rico et al. (2008) and Concha Larrauri & Lall (2018), the newly developed model significantly outperformed the existing models. The author suggested that the deviation observed in the accuracy results of the model is due to the limitations of the key variables considered, noting that tailings characterization has a significant effect on explaining the recorded volume of tailings released upon failure.

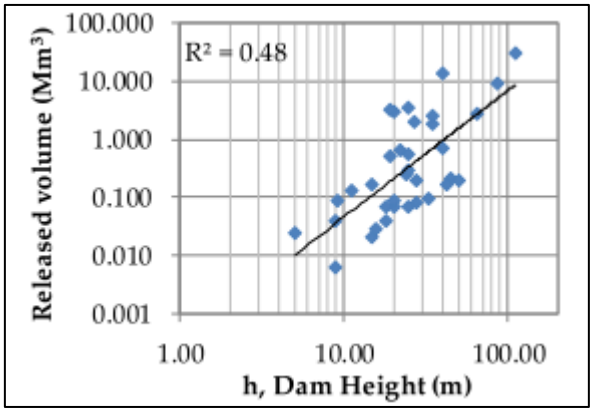

Figure 2-17: The relationship observed between recorded release volume and the dam height at the time of failure, from Quelopana (2019).

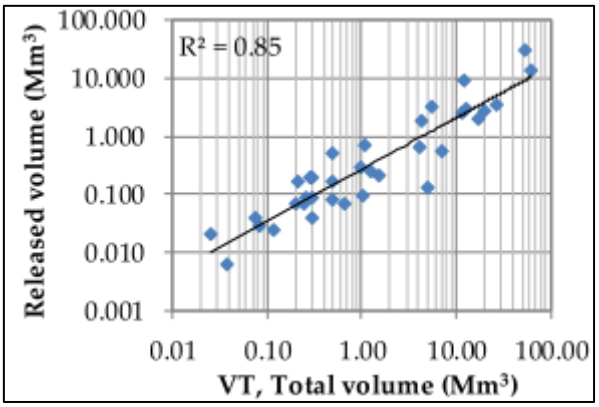

Figure 2-18: The relationship observed between recorded release volume and the impoundment volume, from Quelopana (2019).

Rourke and Luppnow (2015) set out to define the effect of the supernatant pond on the potential release volume of TSFs. Specific mention is made to the empirical relationships developed by Rico et al. (2008) with criticism of the fact that the relationships assume a large total storage volume assumes a larger risk of tailings release. The authors argue the point that a large, well-managed TSFs does not necessarily pose a greater risk than a smaller mismanaged tailings dam and place emphasis on the effect of excess water storage in the supernatant pond. The authors hypothesized that a ratio of pool surface area to impoundment area be related to the breach volume to total volume ratio which aims to determine the effect of the supernatant pond. Rourke & Luppnow (2015) found a very strong relationship between the pool ratio at the time of failure and the recorded magnitude of failure, shown in Figure 2-20.

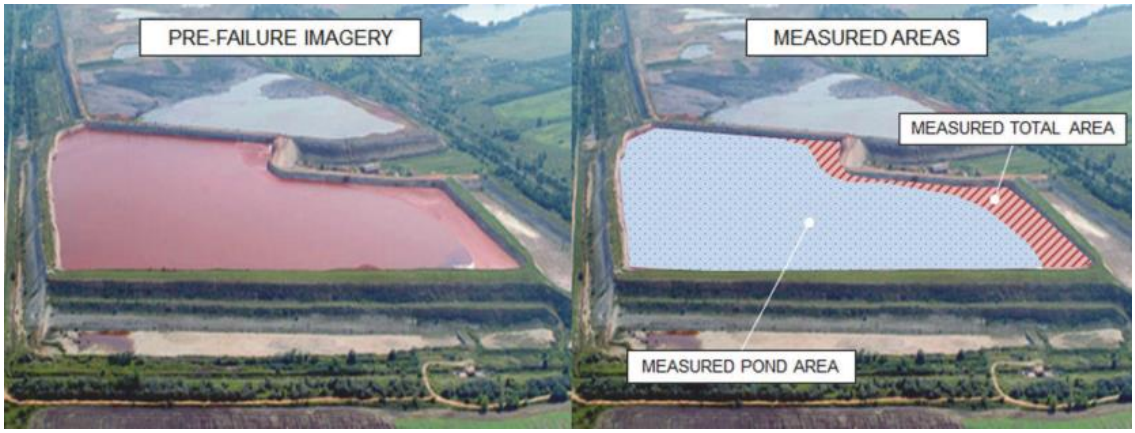

Figure 2-19: Example of supernatant pond surface area determination on the Kolontar tailings dam from Rourke & Luppnow (2015).

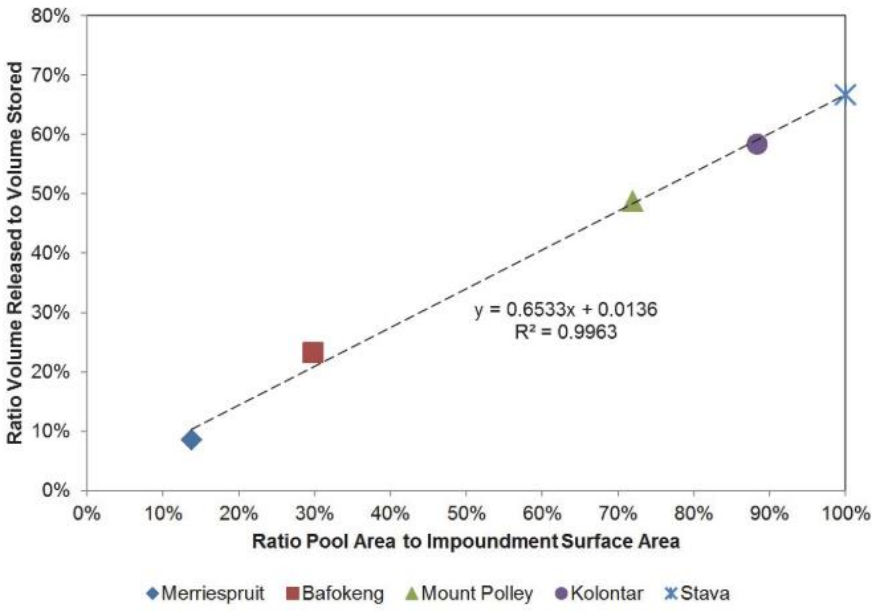

Figure 2-20: Ratio of pool area to impoundment surface area versus the ratio of released tailing volume to total tailings volume from Rourke & Luppnow (2015).

2.6 Summary of Literature Review

From the extensive literature review it was found that upstream type TSFs are more prone to failure than downstream or centreline type TSFs. This is attributed to their weak performance under seismic loading and their sensitivity to phreatic surface migration which leads to the loss of structural stability in the underlying tailings material. The literature review also proved that earthquakes, overtopping, and seepage were the identified failure mechanism for most recorded failures. It has become clear that there are certain characteristics (topography, water content of tailings, breach parameters) that cannot be considered during the TDBA when using the current regression models to predict the potential release volume.

The existing prediction models developed by Rico et al. (2008), Rourke& Luppnow (2015), Concha Larrauri & Lall (2018) and Quelopana (2019) all provided relatively accurate estimations of potential release volume and run-out distance for TSF failures. The estimation models were developed using datasets of varying sizes.

Rico et al (2008) developed their estimation models for potential release volume and run-out distance using 28 cases. The authors' model for estimating the potential release volume achieved a R^2 value of 0.86 by examining the relationship between the total storage volume and recorded release volume. The model developed for estimating the potential run-out distance achieved a R^2 value of 0.57 by examining the relationship between the height of the dam, the recorded release volume, and the recorded run-out distance.

Rourke & Luppnow (2015) set out to examine the relationship between the recorded pool ratio and recorded magnitude of failure of 5 cases. The authors' estimation model achieved a R^2 value of 0.99. The authors showed that there is a strong correlation between the amount of water present at the time of failure and the potential release volume of the TSF.

Concha Larrauri & Lall (2018) developed estimation models based on those developed by Rico et al (2008) by using an updated database consisting of 29 failure cases. The authors introduced a dam factor to quantify the energy associated with the failure, used to during the estimation of potential run-out distance. The model developed for estimating the potential release volume achieved an R^2 value of 0.88 whilst the model for estimating the potential run-out distance achieved a R^2 value of 0.65.

Quelopana (2019) developed an estimation model for estimating the potential release volume by examining the relationship between the height of the dam, the total storage volume and the recorded release volume. The author argued that the total storage volume alone cannot provide a robust estimate of release volume. The model developed by the author for estimating the potential release volume achieved a R^2 value of 0.91 on a dataset of 35 failures.

3 Methodology

This chapter describes the methods employed to compile the failure database that was used to generate the empirical correlations for estimation of breach volume and run-out distance. It describes the selection criteria and important exclusion criteria applied to recorded failure cases. It explains the modelling software used to arrive at the desired empirical correlations and discusses the statistical methods used to evaluate and test the accuracy of the correlations achieved.

When conducting analysis of TSF failures there are important variables that influence the volume of tailings released upon failure, these variables are unique to every TSF (Quelopana, 2019). As shown in section 2.5, there exists relationships between the volume of tailings released and the dam geometric characteristics (V_T, h, Pool Ratio (PR)). Current empirical correlations make use of these geometric characteristics to predict potential release volume and run-out distance. A major limitation experienced whilst compiling failure data was finding cases that not only provided the geometric characteristics but also the type of failure and dam type which are important variables used during cause and effect analysis of the recorded failures. These variables are missing from a majority of the recorded failures found in literature and may be due to mis-reporting, reluctance to share the information from a company standpoint or that the failures were simply not recorded (Rico, Benito, Diez-Herrero, *et al.*, 2008; Bowker and Chambers, 2017).

There have been numerous attempts at compiling a database of global tailings dam failures which summarises modes of failure (seepage, erosion, overtopping, foundation failure etc.), total storage volume, the height of the dam, released volume of tailings, dam construction type (upstream, downstream, centreline, etc.), tailings run-out distance in km and the socio-environmental impacts of the failure. The best and most recent example of such a database is the WMTF database created by Bowker et al (2019).

3.1 Database Creation

The failure data contained in the WMTF database was reviewed with the primary objective being to compile a subset of failure cases that provided the dam geometric characteristics that would allow for the development of empirical correlations to be used for the prediction of potential release volume and maximum run-out distance expected upon failure. Through a process of cross referencing, missing or inconsistent information was updated to ensure the database was as complete as possible. Valuable insight was gained from the studies examined in section 2.5 regarding the various important variables to consider when conducting correlation analysis for TSF failures. The database contains the following information of all failure cases:

- Tailings storage facility name

- Year of failure
- Dam Type
- Dam Fill Material
- ICOLD Classifications
- Mode of Failure
- Meteorological Events associated with failure
- Total Storage Volume
- Volume of Tailings Released
- Dam Height
- Recorded Run-out Distance

These parameters are important when conducting a TBDA to understand the circumstances surrounding a specific TSF failure and highlight possible trends from observed failures. To ensure that the cases used for the correlation analysis are representative of catastrophic failures, the following exclusion criteria was applied:

- Failure cases where any quantitative data was missing (V_T, V_F, h) was omitted from the final database.
- Failure cases that did not have the recorded D_{max} values were omitted from the correlation analysis for D_{max}.
- Only cases that qualify as failures according to ICOLD classifications, shown in Table 3-1, would be used for the analysis.

Table 3-1: ICOLD incident classification, from (ICOLD, 2001)

INCIDENT TYPE	
1A	Failure of an active impoundment
1B	Failure of an inactive impoundment
2A	Accident at an active impoundment
2B	Accident at an inactive impoundment
3	Groundwater issue

From the 355 cases recorded by Bowker et al. (2019), 56 failure cases provided the required quantitative and qualitative information. It was decided that the ICOLD ratings on failure type, dam type and severity of failure would be adopted and applied to each case to ensure homogeneity is kept between references. The database includes 5 failure cases used by Rourke & Luppnow (2015), which in addition

to the total impoundment volume, volume of tailings released and dam height, included the pond ratio at the time of failure. By using Google Earth and through review of available literature sources it was possible to calculate PR values for Kingston fossil plant and Padcal No 3 (cases 25 and 44). Figure 3-1 shows the method employed to determine the pool ratio for the additional cases. A further 9 cases (cases 17, 30, 35, 37, 44, 46, 49, 50 and 51) provided qualitative information regarding meteorological events that occurred prior to failure, events like heavy, prolonged rainfall and snow melt events. This provided valuable qualitative data regarding the possible pond size prior to failure.

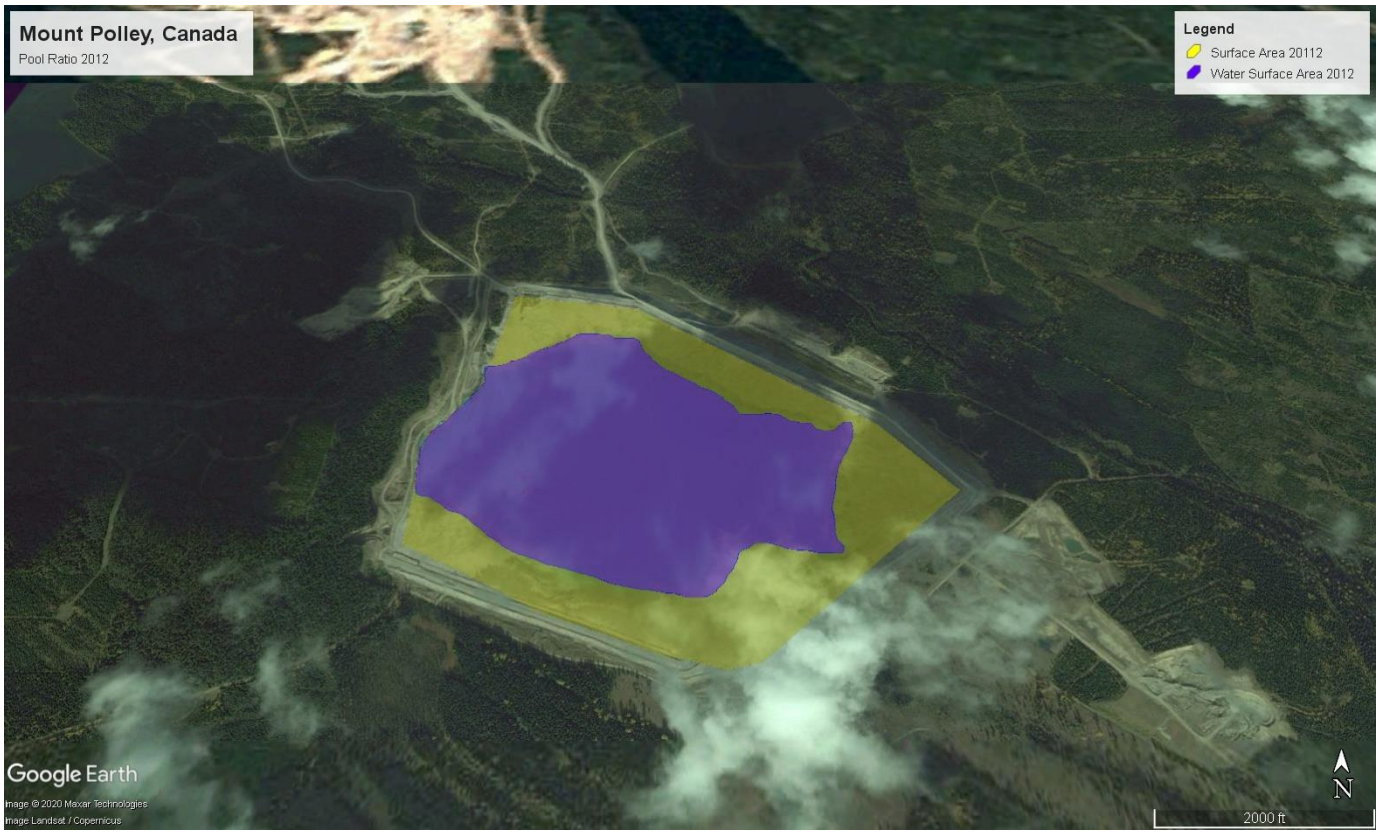

Figure 3-1: Google Earth image of Mount Polley TSF showing the surface area of the ponded water (blue) in 2012 compared to the surface area of the impoundment (yellow). This image was taken to double check of the Pool Ratio measured by Rourke & Luppnow (2015).

Due to the effects that topography and elevation have on the recorded D_{max} values as noted by Rico et al. (2008), it was decided to measure the gradient for the recorded failures which provided pool ratio data in an attempt to correlate the gradient and pool ratio to the D_{max} value. This was done to quantify the effects of the surrounding terrain on the predicted D_{max}. Although this represents only an elementary quantification of the topography of the surrounding terrain, it was deemed worthwhile to assess the influence of gradient on the predicted D_{max}. To calculate the gradient of the recorded failure cases, the flow paths of the failures were first identified from literature sources and available aerial photography. The flow paths observed for the failure cases flowed towards water bodies or dry riverbeds. It was noted that in some failure cases the tailings flow entered surrounding water bodies which caused a greater dispersion than would be expected for a debris flow with such high solid contents. Therefore, it was

decided to measure the gradient over the distance from the centre of the TSF to the nearest water body or natural depression. By using the ruler functionality in Google Earth, elevation paths were drawn for each failure from the centre of the TSF to the nearest water body or natural depression along the observed flow path, an example for Mount Polley is shown in Figure 3-2. The highest and lowest point along the path were identified and the difference between these values was divided by the distance between the two points as measured on the elevation profile shown in Figure 3-2. The gradient for cases 3, 4, 24, 25, 35, 44 and 46 were collected. These cases were selected as there was reliable satellite imagery available and the flow paths were previously defined in literature sources.

$$Gradient = \frac{Elevation\ at\ the\ centre\ of\ the\ TSF - \ Elevation\ at\ the\ lowest\ lying\ point}{Distance\ between\ the\ points}$$

After careful analysis of each failure case through cross referencing with various literature sources, the available information for each failure case was summarised in Table 3-2.

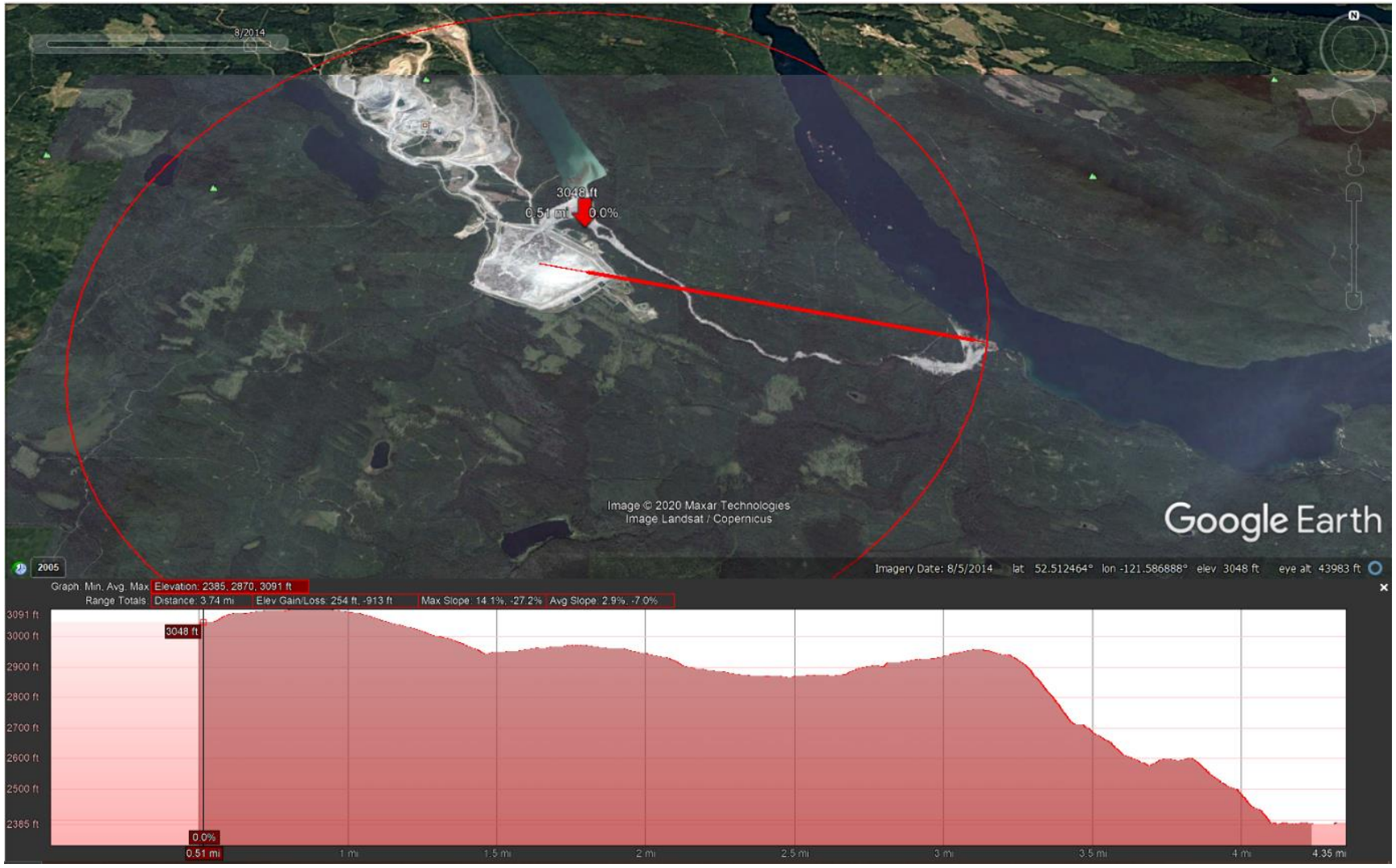

Figure 3-2: Google Earth image showing the flow path along a valley of the Mount Polley TSF failure along with the elevation profile from the centre of the TSF to the point where the flow slide entered Quesnel Lake

Table 3-2: Database of recorded TSF failures (Failure modes: OT= Overtopping, SI= Slope Instability, SE= Seepage, FN= Foundation Failure, EQ= Earthquake, ER= Erosion, NR= Not Reported).

No	Mine	Year	Failure Mode	Height	Impoundment Volume (Vt)	Release Volume (Vf)	Run-out Distance (Dmax)	Gradient	Pool Ratio	Rainfall Event
				(m)	*(Mm^3)*	*(Mm^3)*	*(km)*	*(%)*	*(%)*	
1	(unidentified), Southwestern USA	1973	SI	43.00	0.50	0.17	25.00			
2	Aitik Mine, Sweden	2000	ER	15.00	15.00	1.80	5.20			
3	Ajka Alumina Plant, Hungary	2010	SE	22.00	1.20	0.70	6.00	1.105%	88%	
4	Bafokeng, South Africa	1974	SE	20.00	13.00	3.00	45.00	0.579%	30%	
5	Baia Mare, Romania	2000	NR	7.00	0.18	0.10	0.18			
6	Balka Chuficheva, Russia	1981	SI	25.00	27.00	3.50	1.30			
7	Barahona, Chile	1928	EQ	61.00	20.00	3.78				
8	Bellavista, Chile	1965	EQ	20.00	0.45	0.07	0.80			
9	Buffalo Creek, USA	1972	NR	16.00	0.50	0.50	64.40			
10	Bonsal, USA	1985	OT	6.00	0.04	0.01	0.80			
11	Castano Viejo, Argentina	1964	SE	9.00	0.03	0.02	2.20			
12	Cerro Negro No. (3 of 5), Chile	1965	EQ	20.00	0.50	0.09	5.00			
13	Cerro Negro No. (4 of 5), Chile	1985	EQ	40.00	2.00	0.50	8.00			
14	Churchrock, USA	1979	FN	11.00	0.37	0.37	112.60			
15	Cities Services, USA	1971	SE	15.00	12.34	9.00	120.00			

No	Mine	Year	Failure Mode	Height (m)	Impoundment Volume (Vt) (Mm^3)	Release Volume (Vf) (Mm^3)	Run-out Distance (Dmax) (km)	Gradient (%)	Pool Ratio (%)	Rainfall Event
16	Consolidated Coal No. 1, USA	1988	OT	85.00	1.00	0.25				
17	Deneen Mica, USA	1974	SI	18.00	0.30	0.04	0.03			Heavy Rain
18	El Cobre New Dam, Chile	1965	EQ	19.00	0.35	0.35	12.00			
19	El Cobre Old Dam, Chile	1965	EQ	35.00	4.25	1.90	12.00			
20	Fundao (Germano), Brazil	2015	ST	90.00	55.00	43.00	637.00			
21	Hokkaido, Japan	1968	EQ	12.00	0.30	0.09	0.15			
22	Huayuan County, China	2009	U	10.00	0.05	0.05				
23	Huogudu, China	1962	U	19.00	5.42	3.30				
24	Mt Polley, Canada	2014	FN	40.00	74.00	23.60	7.00	2.874%	72%	
25	Kingston fossil plant,USA	2008	U	18.00	15.29	4.10	4.10	2.038%	32%	
26	Kokoya Gold Mine, Liberia	2017	U	25.00	0.30	0.01				
27	La Luciana, Spain	1960	SI	24.00	1.25	0.25				
28	Las Palmas, Chile	2010	EQ	15.00	0.22	0.17				
29	Lixi Tailings Dam, China	2008	U	50.70	0.29	0.27	2.50			
30	Los Cedros, México	1937	ST	15.00	9.20	2.50	11.00			Heavy and prolonged rainfall
31	Los Frailes, Spain	1998	FN	27.00	15.00	6.80	41.00			
32	Los Maquis No. 3	1965	EQ	15.00	0.04	0.02	5.00			

No	Mine	Year	Failure Mode	Height	Impoundment Volume (Vt)	Release Volume (Vf)	Run-out Distance (Dmax)	Gradient	Pool Ratio	Rainfall Event
				(m)	*(Mm^3)*	*(Mm^3)*	*(km)*	*(%)*	*(%)*	
33	Madjarevo, Bulgaria	1975	ST	40.00	3.00	0.25	20.00			
34	Maritsa Istok 1, Bulgaria	1992	ER	15.00	52.00	0.50				
35	Merriespruit, South Africa	1994	OT	31.00	7.04	0.60	4.00	1.440%	14%	Heavy Rain
36	Middle Arm, Tasmania	1995	OT	4.00	0.03	0.01				
37	Mike Horse, USA	1975	OT	18.00	0.75	0.15				Heavy Rain
38	Mina Córrego do Feijão (San Brumadinho), Brazil	2019	U	110.00	12.00	11.70	8.00			
39	Mochikoshi Dike No 1 (1 of 3), Japan	1978	EQ	28.00	0.48	0.08	8.00			
40	Mufulira, Zambia	1970	MS	50.00	1.00	0.07				
41	Niujialong	1985	OT	40.00	1.10	0.73				
42	Olinghouse, USA	1985	SE	5.00	0.12	0.03	1.50			
43	Omai Mine, Guyana	1995	ER	44.00	5.25	4.20	80.00			
44	Padcal No 3, Philippines	2012	OT	30.00	102.00	13.00		11.609%	29%	Heavy Rain
45	Partizansk, Russia	2004	U	20.00	20.00	0.16				
46	Stava, Italy	1985	SI	29.50	0.30	0.19	4.20	13.044%	100%	Heavy Rain
47	Riltec, Tasmania	1995	SE	7.00	0.12	0.04				

No	Mine	Year	Failure Mode	Height	Impoundment Volume (Vt)	Release Volume (Vf)	Run-out Distance (Dmax)	Gradient	Pool Ratio	Rainfall Event
				(m)	*(Mm^3)*	*(Mm^3)*	*(km)*	*(%)*	*(%)*	
48	Sasa Mine, Macedonia	2003	ST	25.00	2.00	0.09	12.00			
49	Sgurigrad, Bulgaria	1966	SI	45.00	1.52	0.22	6.00			Heavy and prolonged rainfall
50	Silver King, USA	1974	OT	9.00	0.04	0.01				Snowmelt
51	Stancil, USA	1989	SI	9.00	0.07	0.04	0.10			Heavy Rain
52	Tuba, Philippines	1992	FN	25.00	40.49	32.24				
53	Tyrone (Phelps Dodge), USA	1980	SI	66.00	2.50	2.00	8.00			
54	Veta de Agua	1985	EQ	24.00	0.70	0.28	5.00			
55	Veta del Agua No5	2010	EQ	16.00	0.08	0.03				
56	Zletovo No. 4, Yugoslavia	1976	SI	25.00	1.00	0.30				

3.2 Modelling Software

Eureqa modelling software was chosen to examine the relationships between the physical characteristics of the TSF listed in Table 3-2. Eureqa is a Artificial Intelligence (A.I.) powered modelling engine developed by the Computational Synthesis Lab at Cornell University. Eureqa uses symbolic regression to detect equations and hidden mathematical relationships that may exist in raw data by implementing a similar algorithm to Lipson's algorithm for self-contemplating robots (Dubčáková, 2011). Symbolic regression is a type of regression analysis that searches for a model that is in its simplest form and best fits the given database. Data can be entered directly into Eureqa whereafter the user can perform a series of data manipulations to smooth and remove outliers that may be present. The user can then define the form of the desired function and set the dependent variable. Once a best fit relationship has been defined the error metrics are available as the R^2 value, Mean Absolute Error or Mean Squared Error.

3.3 Data Setup and Modelling

Once all failure cases were compiled into Table 3-2, the geometric characteristics could be used to complete the correlation analysis for the given failure cases. The correlation analysis was done using Eureqa modelling software for both V_F and D_{max} based on different cases that will be discussed below. The forms of the various equations were selected to be comparable to previous works done. It was found that power functions performed the best when examining the complex relationships between the various parameters. The results will be discussed in Chapter 4.

3.3.1 Release Volume (V_F):

To estimate V_F from the data contained in Table 3-2, it was decided that two separate analyses would be conducted. One utilising the entire database of 56 cases (approach V_F.1) and a second on the 7 cases which presented PR data (approach V_F.2). Due to the nature of the failure data, it was decided to include outliers in the modelling datasets as to ensure the developed models remain representative of the size ranges of TSF. For approach V_F.1 the correlation was set to be a function of V_T, V_F and h, building on the correlations developed by Rico et al. (2008), Concha & Lall (2018) and Quelopana (2019). The model was run with a 50% training and 50% validation data criteria. The model was to take the following form shown in Eq. 2, with ρ, σ and τ being calibration constants assigned by Eureqa.

$$V_F = \rho \times V_T^{\sigma} \times h^{\tau} \qquad \textit{Eq. 2}$$

For approach V_F.2, the 7 cases (3, 4, 24, 25, 35, 44 and 46) from Table 3-2 that presented PR values were imported to Eureqa, the correlation was set to be a function of V_T, V_F and PR to examine the impact of the pool ratio on the release volume. It was found that the analysis provides a better approximation and simpler syntax when comparing the pool ratio to the magnitude of failure (V_F/V_T) due to the smaller dataset used for training. The model was run with a 50% training and 50% validation data criteria. The function was set to take the form shown in Eq. 3.

$$\frac{V_F}{V_T} = \alpha PR + \beta \qquad \textit{Eq. 3}$$

3.3.2 Run-out Distance (D_{max}):

A similar methodology was followed to estimate D_{max} as was followed for the estimation of V_F. Two separate analyses were conducted, one utilising the 37 cases from Table 3-2 which presented D_{max} values (approach D_{max}.1) and a second on the 7 cases which presented PR data (approach D_{max}.2). For approach D_{max}.1 the correlation was set to be a function of D_{max} and H_f continuing the work done by Concha & Lall (2018). The D_{max} and H_f variable data was imported to Eureqa. The model was run with a 50% training and 50% validation data criteria. The model was set to take the form of a power function with calibration constants α and β, as shown in Eq. 4:

$$D_{max} = \alpha H f^{\beta} \qquad \textit{Eq. 4}$$

For approach D_{max}.2, the 7 cases (3, 4, 24, 25, 35, 44 and 46) from Table 3-2 that presented PR values were imported to Eureqa, the correlation was set to be a function of D_{max}, PR, gradient (GR) and H_f. The model was run with a 50% training and 50% validation data criteria. This model will be a first attempt at quantifying the effect of local topography on the run-out distance of a tailings flow. The model was defined to have the following form shown in Eq. 5.

$$D_{max} = \propto PR^{\delta} GR^{\gamma} V_f^{\beta} \qquad \textit{Eq. 5}$$

3.4 Testing

Testing of the relationships derived for predicting V_F and D_{max} were done against the existing empirical correlations developed by Rico et al. (2008), Rourke & Luppnow (2015), Concha & Lall (2018) and Quelopana (2019). Each variable was tested in their own respect as predicted versus observed values to determine the model's comparative performance in relation to existing models. The error metrics used to compare the accuracy of each model were chosen to be the R^2 value and the RMSE. RMSE is defined as the standard deviation of the residuals for a given dataset, and is a measure of the average distance of the residuals from the line of best fit with the same units of measure as the dependent variable (Barnston, 1992).

The correlations developed for estimation of V_F and D_{max} which are a function of the PR prior to failure were back tested against the case studies which provided qualitative data regarding water conditions prior to failure. A total of 9 cases provided the required qualitative data, 3 of the cases (cases 35, 44 and 46) were already used during the regression analysis. The remaining 6 cases (cases 17, 30, 37, 49, 50 and 51) experienced heavy rain prior to failure, heavy and prolonged rain prior to failure and snow melt events where run-off water would collect on the surface of the tailings dam, but did not provide PR data.

- Heavy rain events as described were taken as referring to sudden large amounts of water ponding on the surface of the TSF. These cases were associated with overtopping and slope instability failure modes.
- Heavy, prolonged rain events were taken to be large amounts of rain that have had time to seep into the tailings material thus saturating the tailings. These cases were associated with structural failures.

It was decided to back test the model using these 6 cases and estimate their respective PRs prior to failure. The estimated PR would then be compared to the 3 cases that provided both PR and meteorological data to determine whether the model provides realistic results. The model developed for approach V_f.2 would be rearranged to estimate the PR prior to failure. Cases 35, 44 and 46 had PRs ranging between 14% and 100%, with the average PR for these cases being 48%. It was hypothesized that cases that experienced heavy rainfall prior to failure would have estimated PRs higher than 30%. This value was chosen as a conservative value to represent a TSF pool ratio after a period of heavy rainfall considering that adequate water displacement measures would be in place. This value however is subjective and should be taken as a first round validation to ascertain whether the model has merit.

4 Results and Discussion

This chapter presents the results obtained after completing the correlation analysis and modelling for V_F and D_{max} using the data contained in Table 3-2. The results are presented in the order outlined in section 3.2, first the models developed for the estimation of V_F using approach $V_F.1$ and $V_F.2$ will be presented followed by the models developed for the estimation of D_{max} using approach $D_{max}.1$ and $D_{max}.2$. The accuracy of each model will be tested against the applicable existing models and are discussed in each respective section.

4.1 Estimation of V_F

The quantitative data contained in Table 3-2 was used to determine the relationships between the dam geometric characteristics and the recorded release volume and run-out distances. For each model the relationships between the individual dam characteristics were examined to determine their correlations to each other, these relationships will be shown in the Appendices.

4.1.1 Approach V_F .1:

The power function indicated by Eq. 2 was used in the modelling process to complete the estimation of V_F for approach $V_F.1$ utilising the full database of 56 cases to analyse the relationship between V_F, V_T and h. Appendix C.1 shows the relationship between the impoundment volume and recorded release volume with a power trendline and a slight dispersion between the data points, and is plot on a log scale for all cases contained in Table 3-2. Appendix C.1 also shows the relationship between the height of the TSF and the recorded release volume with a power trendline and presents a slight correlation and larger dispersion in data points. A decrease in the R^2 values was observed for V_F to V_T and V_F to h with values 0.79 and 0.32 respectively when compared to the values obtained by Quelopana (2019) on his own dataset, of 0.85 and 0.45 respectively. This was attributed to the increase in data points used to examine the relationships between these geometric characteristics.

After examining the relationships between the dam geometric characteristics, the data from Table 3-2 was imported to Eureqa. Eq. 6 shows the result after training and validation on the data in Eureqa with the calculated calibration constants, hereafter referred to as model $V_F.1$.

$$V_F = 0.0742 \times V_T^{0.763} \times h^{0.654} \qquad \textit{Eq. 6}$$

Figure 4-1 shows the recorded V_F values contained in the database compared to the predicted V_F values obtained by implementing the model $V_F.1$. The accuracy of the developed model was measured against the current empirical correlations developed by Rico et al (2008), Concha & Lall (2018) and Quelopana (2019). Data points plotting above the recorded failures trendline were overestimated using the empirical models whilst these plotting below the trendline were underestimated. The data points that were overestimated indicate a larger dispersion than these that were underestimated. This may be attributed to the confidence bounds associated with each empirical model.

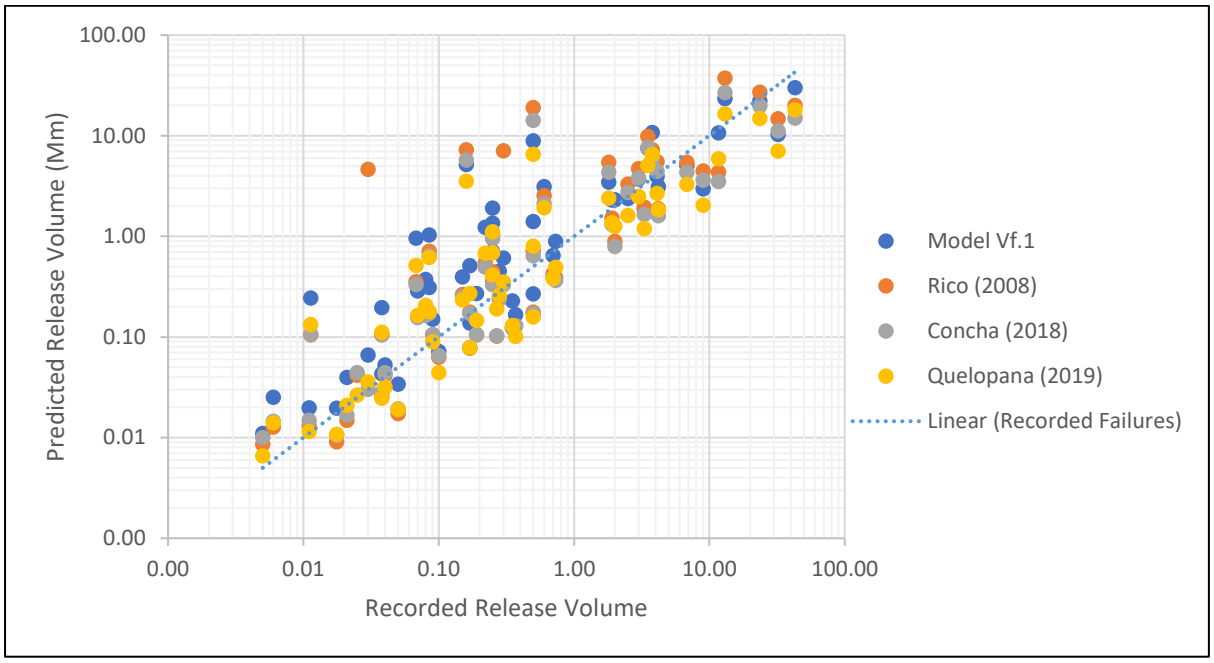

Figure 4-1: Recorded V_F vs predicted V_F for current prediction models available as tested against the dataset in Table 3-2.

Table 4-1 summarises the R^2 and RMSE values obtained from model V_F.1 compared to the other empirical models as discussed in section 2.5. To ensure a representative comparison was made, the models were tested against the entire database in Table 3-2 where after the developed model was tested against each corresponding authors cases that was contained in Table 3-2. Model V_f.1 performed better than the existing prediction models when applied to the failure cases in Table 3-2, achieving a R^2 value of 0.72 and RMSE of 1.207 Mm^3. The model also performed well when applied to the common cases selected from the authors' databases. Model V_F.1 consistently achieved a lower RMSE value than the corresponding existing models when juxtaposed to the selected cases from previous work done.

Table 4-1: Accuracy of developed model using approach 1 for estimation of V_F compared to current prediction models.

Cases	Model V_f.1		Rico (2008)		Concha & Lall (2018)		Quelopana (2019)	
	R^2	RMSE	R^2	RMSE	R^2	RMSE	R^2	RMSE
All Cases	0.72	1.207	0.46	1.347	0.48	1.048	0.69	4.308
Rico (2008)	0.49	1.696	0.50	1.819	-	-	-	-
Concha & Lall (2018)	0.94	3.047	-	-	0.74	5.790	-	-
Quelopana (2019)	0.92	2.811	-	-	-	-	0.91	4.876

After analysis of the prediction bounds of model V_f.1, it was evident that the model provides a more accurate prediction for failure cases with recorded release volumes greater than 1 Mm^3. The model provides a less accurate but a more conservative prediction for cases with recorded release volumes lower than 1 Mm^3. Overall, model V_F.1 performed better than the most recent empirical model developed by Quelopana (2019) when applied to the new, larger database of failures in Table 3-2. Model

V_f.1 achieved a higher R^2 value and a much lower RMSE value than the model developed by Quelopana (2019). When the model was test against the cases from Rico et al (2008), a lower R^2 value was achieved than the existing model. Model V_f.1 however achieved a lower RMSE value than the model developed by Rico et al (2008). The higher R^2 value and low RMSE value achieved by model V_f.1 compared to the performance of the existing models suggests an improvement in the estimation of V_f, albeit a marginal increase. This improved empirical model provides a better approximation of release volume based on basic dam geometric characteristics (V_t, h).

4.1.2 Approach V_F .2:

For cases 3, 4, 24, 25, 35, 44 and 46, which presented PR data, another set of relationships were derived. A strong linear relationship was observed between the magnitude of failure (V_F/V_T) and the PR at the time of failure. Approach V_F.2 utilised these 7 cases to examine the relationship between V_F, V_T and PR. The relationship derived is shown by Eq. 7 and has a R^2 value of 0.98 and an RMSE of 0.04 Mm^3, hereafter referred to as model V_F.2. The accuracy of model V_F.2 was tested against the model developed by Rourke & Luppnow (2015) with the recorded V_F compared to the predicted V_F shown in Figure 4-2. Table 4-2 summarises the R^2 and RMSE values obtained for model V_F.2 and the model developed by Rourke & Luppnow (2015). The models performed equally well with model V_F.2 being developed on a slightly larger dataset. A major limitation experienced when developing model V_F.2 was the availability of pre-failure pool ratio data.

$$\frac{V_F}{V_T} = 0.875PR^{0.868} \times h^{-0.097} \qquad \textit{Eq. 7}$$

Table 4-2: Accuracy of the model developed using approach 2 compared to the model developed by Rourke & Luppnow (2015).

	Model V_f.2		**Rourke & Luppnow (2015)**	
	R^2	***RMSE***	***R^2***	***RMSE***
Cases 3, 4, 24, 25, 35, 44 and 46	0.98	0.04	0.97	0.04

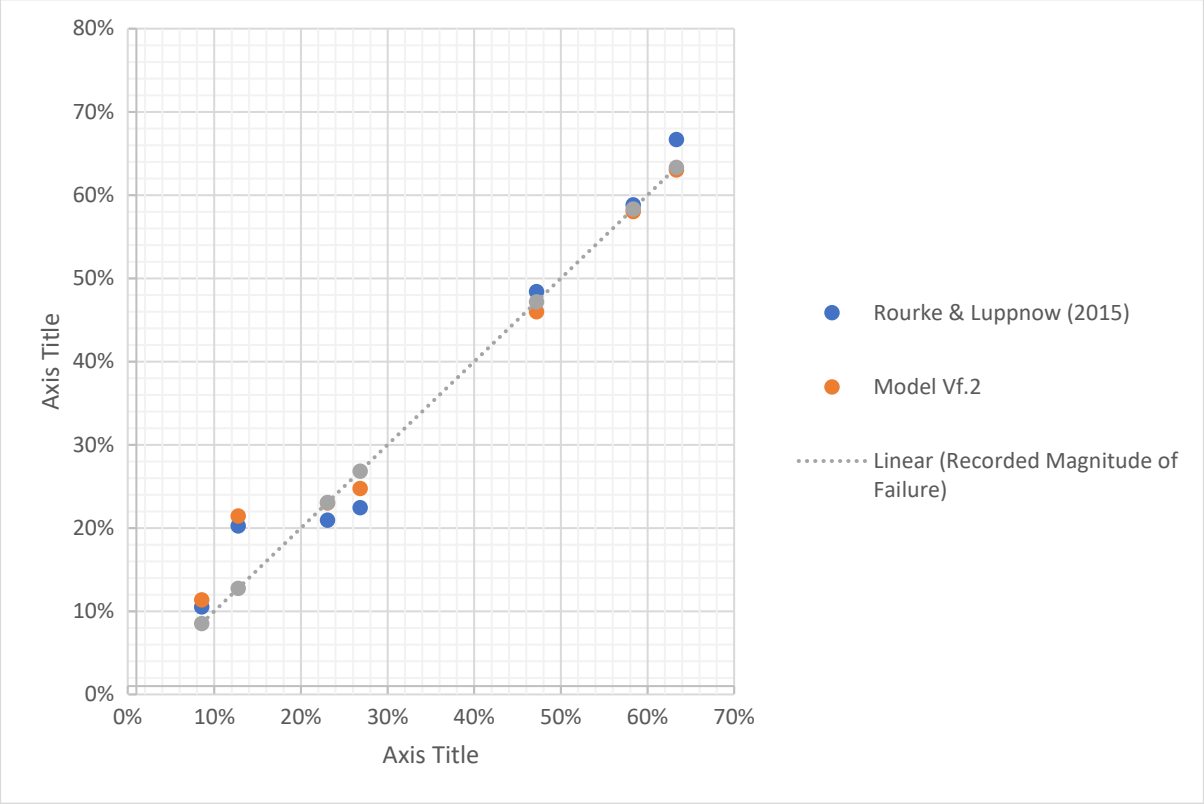

Figure 4-2:Recorded V vs predicted V of the model developed using pool ratio compared to the model developed by Rourke & Luppnow (2015).

Figure 4-2 shows the recorded magnitude of failure compared to the predicted magnitude of failure achieved using model $V_f.2$. The model provides an accurate prediction for magnitude of failures greater than 40% and a conservative prediction for failure cases with magnitudes of failure less than 40%. Model $V_f.2$ is seen as an improvement to the empirical model developed by Rourke & Luppnow (2015) as more data points were used to train the model. The model strengthens the argument that the size of the supernatant pool prior to failure has a direct impact on the potential release volume and therefor warrants further research to improve on the current empirical relationship.

Table 4-3 shows the results of back testing using model $V_f.2$ to estimate the pool ratio prior to failure of cases providing qualitative data of meteorological events prior to failure. The pool ratio estimations fall within a range of 15% to 69%. This falls within the range of recorded PR values for cases 35, 44 and 46 (14% to 100%). Only two cases (30 and 51) have estimated PRs greater than the hypothesized 30% PR associated with large hydrological events. The remaining cases had estimated PRs that are lower than 30%, ranging from 15% to 25%. From this back testing it is evident that model $V_f.2$ provides a good estimation of the magnitude ratio as the estimated PRs fall within a realistic range comparable to the observed PRs.

Table 4-3: Back testing of model V_f.2 to predict pool ratio.

	Failure Case	Year	Failure Mechanism	Height (m)	Magnitude Ratio	Predicted PR	Rainfall Event
17	Deneen Mica, USA	1974	SI	18	13%	15%	Heavy Rain
30	Los Cedros, México	1937	ST	15	27%	35%	Heavy, Prolonged rainfall
37	Mike Horse, USA	1975	OT	18	20%	25%	Heavy Rain
49	Sgurigrad, Bulgaria	1966	SI	45	14%	19%	Heavy, Prolonged rainfall
50	Silver King, USA	1974	OT	9	16%	18%	Snowmelt
51	Stancil, USA	1989	SI	9	51%	69%	Heavy Rain

4.2 Estimation of D_{max}

4.2.1 Approach D_{max} .1:

Approach D_{max}.1 utilised 37 cases from Table 3-2 that provided recorded D_{max} values. An important factor to consider when assessing the run-out distances of TSF failures is the presence of waterways and dry riverbeds. Topographical and hydrological settings greatly influence the lateral extent of the tailings flow. For instance, upon failure of a valley impoundment, the tailings flow is constricted and concentrated to flow further downstream. These factors cannot be accounted for in the empirical models developed and used during this analysis.

Appendix C.2 shows a power function correlation between recorded D_{max} values and the predictor H_f with a large dispersion of datapoints. The relationship suggests that D_{max} is proportional to V_F, h and the magnitude of failure as H_f is defined as a function of these three variables. H_f proved to be the most reliable variable for use in D_{max} estimations and therefore the correlation was assessed and compared to the models developed by Concha Larrauri & Lall, (2018) and Rico et al. (2008) using the new database. The relationship derived after modelling in Eureqa is shown in Eq. 8, hereafter referred to as model D_{max}.1, and has a R^2 value of 0.81 and RMSE of 47.77 km.

$$D_{max} = 0.0457 Hf^{1.19} \qquad \textit{Eq. 8}$$

.

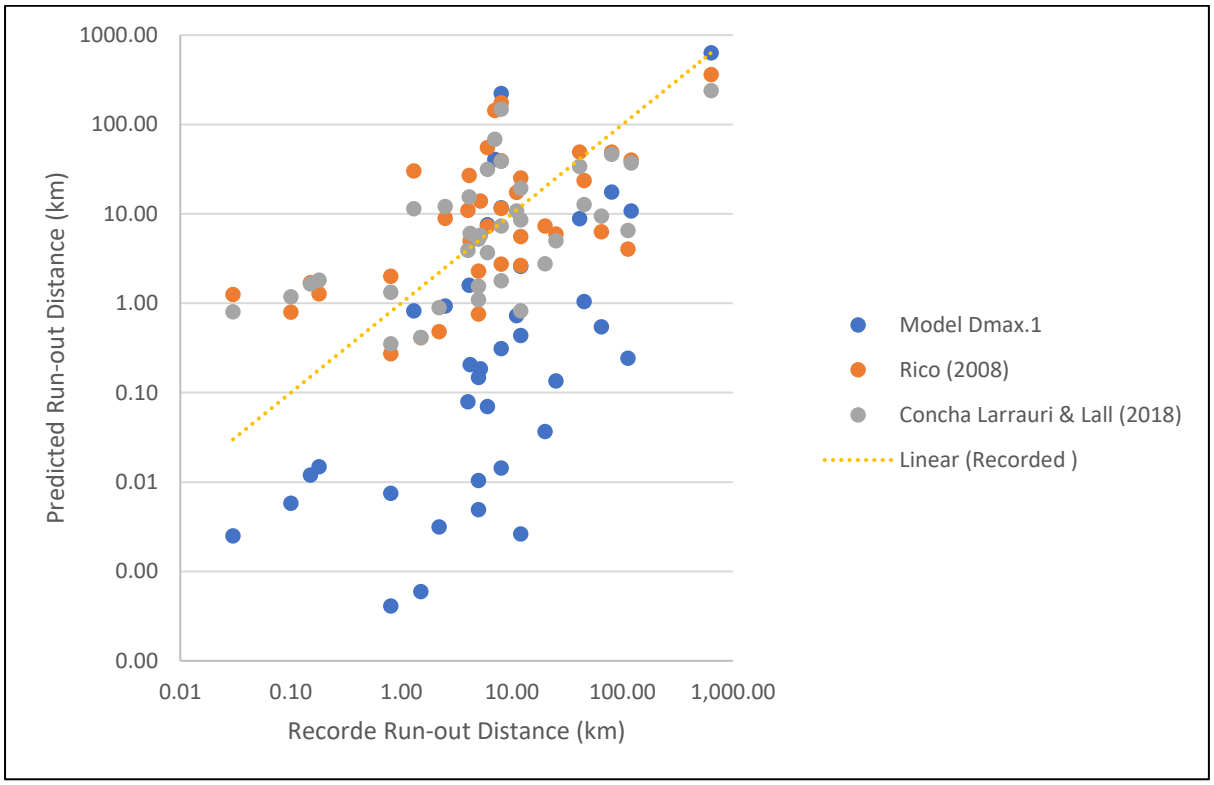

Figure 4-3:Recorded run-out distance vs predicted run-out distance for current prediction models available as tested against the 37 cases providing Dmax values in Table 3-2.

Table 4-4 summarises the R^2 and RMSE values obtained for model $D_{max}.1$ compared to the models developed by Rico et al (2008) and Concha & Lall (2018).

Table 4-4: Accuracy of model $D_{max}.1$ compared to previously developed models.

Data	Model $D_{max}.1$		Rico (2008)		Concha & Lall (2018)	
	R^2	RMSE	R^2	RMSE	R^2	RMSE
All Cases	0.81	47.777	0.66	64.043	0.64	74.882
Rico (2008)	0.34	19.217	0.24	19.830	-	-
Concha & Lall (2018)	0.93	35.343	-	-	0.88	82.421

From Figure 4-3, it is evident that model $D_{max}.2$ underestimates the run-out distance for the majority of the datapoints. The dispersion of points is attributed to the uncertainty of the presence of rivers and valleys that cannot be considered in the model. Google earth images reveal that most cases flowed into rivers and or valleys which greatly exaggerates the lateral extent of the tailings flow. This can be seen in the large range of the recorded run-out distances (0.03 km to 637 km). The approach to estimating D_{max} needs to be refined to account for cases where the tailings flow reached a water body.

4.2.2 Approach D_{max} .2:

Approach Dmax.2 would be a first attempt at quantifying the effect of the gradient along the most likely flow path on the run-out distance. The model was set to take the form defined in Eq. 5. The PR and

Gradient variables were chosen along with the VF values to estimate the Dmax for the failure cases. The relationship derived after modelling in Eureqa is presented by Eq. 9, hereafter referred to as model Dmax.2. Model Dmax.2 achieved a R2 value of 0.77 and a RMSE of 3 km. The predicted Dmax values calculated by model Dmax.2 is compared to the recorded Dmax values are shown in Figure 4-4. The model severely underpredicts 3 cases' Dmax values, this is attributed to the limited datapoints used for model training which influences the stability of the developed model. The range of recorded Dmax values used for the development of this model was 4 km to 15 km, with an average of 6.61 km. The 50/50 training to validation split would mean that a bias would exist which would favour the points used for training. Every effort was made to ensure the training data was randomly selected.

$$D_{max} = \frac{0.0059 V_F}{PR^{1.15} GR^{1.05}} \qquad \textit{Eq. 9}$$

The model provided good estimations for 4 of the seven cases (cases 4, 24, 25 and 35). The model performed well for a majority of the datapoints, with more datapoints the relationship could be further examined with the hopes of developing a robust model for future use.

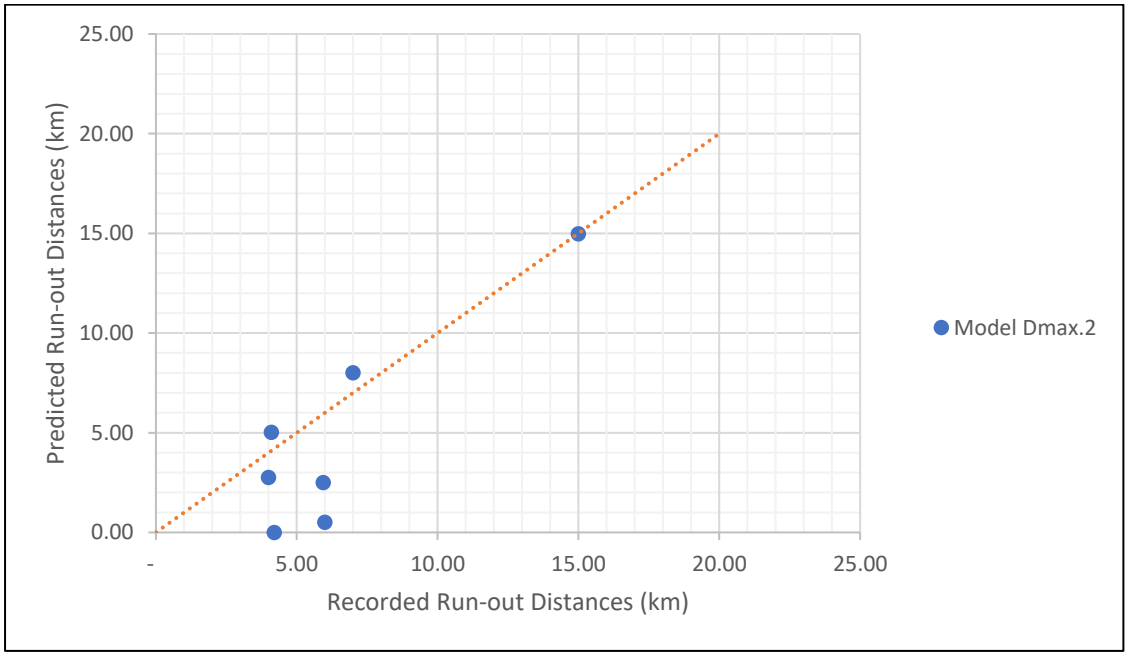

Figure 4-4: Recorded D_{max} compared to the predicted D_{max} values calculated with model D_{max}.2, the orange line represents a 1:1 ratio.

4.2.3 External factors influencing D_{max}

When conducting estimations of potential D_{max} it is important to note that the TSF geometric characteristics alone cannot be used to provide a reliable estimation. After conducting the analysis using model D_{max}.1, it was found that the model under predicted a majority of the failure cases run-out distances. This was not unique to model D_{max}.1 but was seen for the models developed by Rico et al (2008) and Concha Larrauri & Lall (2018) as well, albeit not as pronounced. The variance in the estimated D_{max} values could be attributed to external factors influencing the lateral extent of the run-out. To investigate the possible factors influencing the run-out distance, three cases were identified and

assessed in their own right to identify any possible similarities or differences in failure scenarios. The cases were chosen by taking the cases with the smallest run-out distance, the median run-out distance and the largest run-out distance. These cases were identified to be Deneen Mica, Los Frailes and Fundao respectively (cases 17, 20 and 31).

The Deneen Mica TSF failure had a recorded D_{max} of 0.03 km and a V_f of 0.038 Mm^3. The failure occurred after a heavy rain spout which resulted in the overtopping of the embankment. The recorded water content of the tailings was between 51% to 64% (Brumund, 1984). It was reported that the tailings material involved in the failure did not liquefy, the embankment slumped, and the spilled tailings was deposited into a dry riverbed. The relatively low water content of the tailings material greatly lowered the liquefaction potential of the material and hence limited the run-out distance recorded.

When considering the Los Frailes TSF failure in Spain, the released tailings flowed 3 km over farmlands and into the Agrio river. The recorded D_{max} was 41 km downstream from the TSF, from pre failure photographs it can be seen that the TSF had a significant supernatant pond present (ICOLD, 2001). This validates the assumption that the tailings material was fully saturated. The D_{max} was greatly distorted due to the fact that the material flowed into a river which aids in the dispersion of the tailings material.

Similar to the Los Frailes failure, the Fundao tailings spill flowed into the Gualaxo do Norte river which feeds into the Doce river and subsequently entered the Atlantic Ocean, 637 km away. This recorded D_{max} is not representative of the actual run-out distance, as 80% of the tailings material was deposited within a 120 km radius of Bento Rodrigues (Carmo *et al.*, 2017). Another factor which contributed to the lateral extent of the tailings flow was the fact that the TSF was built as a valley impoundment. The valley would act to concentrate the tailings flow. The gradient between the TSF and Bento Rodrigues was measured to be 2% decline using Google Earth.

From these three very different case studies it can be seen that external factors such as the proximity to a water body, the type of terrain where the TSF is built, and the water content of the tailings material all impact the potential run-out distance of a TSF. This proves that the estimation of potential D_{max} cannot be a function of the TSF geometric characteristics alone but should rather follow a site specific approach to identify factors such as topography, location, and presence of vegetation that might influence the run-out distance.

Table 4-5: Summary table of failure cases with descriptions of factors associated with varying run-out distances.

Case No.	Mine Name	Recorded D_{max} (km)	Did the tailings flow enter a water body[4]?	Gradient of flow path	Surrounding Area
17	Deneen Mica, USA	0.03	No, the slumped tailings came to rest in a dry riverbed	-1%	Low relief countryside, small creek close to TSF, scattered woodland
20	Fundao, Brazil	637	Yes, the released tailings flowed down the valley (approximately 7 km) and into the Doce river which subsequently flowed into the Atlantic Ocean.	-2%	Mountainous area, TSF constructed across a valley
31	Los Frailes, Spain	41	Yes, the released tailings flowed over 2.97 km of farmlands into the Agrio river.	0%	Low relief farmlands, small river close to TSF

[4] Water body refers to any river or lake in the proximity of the TSF.

4.3 Summary of Results

Four models were developed to estimate the potential release volume and run-out distance using the failure database in Table 3-2.The results of this thesis is summarised in Table 4-6. The results discussed in this chapter show that existing models can be improved on by adding more relevant failure data. Model V_f.1 performed better than the corresponding existing models for the estimation of potential V_f. It achieved a higher R^2 value and lower RMSE which equates to a marginally more accurate estimation model. Model V_f.2 achieved a high R^2 value and a very low RMSE when compared to the existing estimation model developed by Rourke & Luppnow (2015). The model highlighted the need to consider the size of the supernatant pond when conducting potential V_f estimations. Model D_{max}.1 achieved a high R^2 value but has a large RMSE value, albeit lower than the existing estimation models' RMSEs. The model severely underpredicted the run-out distance for most of the failure cases compared to the existing estimation models. Model D_{max}.2 performed well given the limited dataset and the fact that it was a first attempt at quantifying topography for an estimation model. The model encountered problems when splitting the data into training and validation sets due to the low number of failures cases available.

Table 4-6: Summary of models developed with performance metrics

Model	Formula	R^2	RMSE	No. of Cases used
V_F.1	$V_F = 0.265 V_T^{0.798} h^{0.098}$	0.72	1.207	56
V_F.2	$\frac{V_F}{V_T} = 0.875 PR^{0.868} \times h^{-0.097}$	0.98	0.035	7
D_{max}.1	$D_{max} = 3.91 Hf^{0.272}$	0.81	47.77	37
D_{max}.2	$\mathrm{D_{max}} = \frac{0.0059 \mathrm{V_F}}{\mathrm{PR^{1.15} GR^{1.05}}}$	0.77	3.000	7

5 Conclusion and Recommendations

The primary aim of this thesis was to compile an updated database of recorded TSF failures that provided the required dam geometric characteristics and released tailings flood characteristics, so as to conduct statistical regression analyses on recorded TSF failures to develop empirical models for estimating potential release volume and run-out distance for a TSF. For the database a total of 56 cases were found to provide the necessary failure information which were used to conduct a statistical regression on the TSF failure geometric characteristics.

Models V_f.1, V_f.2 and D_{max}.1 performed well against current existing empirical models. The increased amount of training data allowed for an increase in the accuracy of the models, especially in model V_f.1 where a significant decrease in the RMSE was seen. The following conclusions can be drawn from the model development:

- Model V_f.1 performed better than previously developed models and achieved a smaller RMSE than previous models. This is attributed to the use of a larger database during the development of the model.
- Model V_f.2 performed slightly better than the model developed by Rourke & Luppnow (2015) with more failure cases used in the development of the model. The model was defined to be a power function that takes the pool ratio prior to failure and the height of the dam into account.
- Model D_{max}.1 performed better than the existing models for estimating the run-out distance when looking at the R^2 and RMSE values. The model however, underpredicted most failure cases. This was attributed to the large variance in values used for training, the fact that only the potential energy of the TSF is considered and that site-specific characteristics such as topography, tailings water content and tailings rheology is not included in the estimation model.
- Model D_{max}.2 performed well with a relatively small RMSE of 3 km. The model is a first attempt at quantifying the effect of local topography by means of incorporating the gradient along the most likely flow path. The model proved that further research into the effect of topography on run-out distance is warranted.

These models provide tailings engineers with the ability to make preliminary estimations as to the downstream risks posed by operational TSFs. The data required (V_t, h) to conduct these estimations can be gathered with relative ease from national dam databases and satellite imagery.

Important lessons learnt from the model development and literature review:

- To perform an accurate estimation of tailings flood characteristics, site specific conditions such as tailings rheology, local topography and breach mechanisms should be considered in the model. Empirical relationships cannot accommodate these specific characteristics and should therefor only be used as a first approximation of the risk and hazard posed by a TSF.

- When estimating D_{max}, it is important to note that factors such as local topography, proximity of TSF to a water body, and the water content of the tailings have an impact on the actual D_{max}. The estimation therefore cannot be taken as only a function of the potential energy of the tailings material as described by the predictor H_f.

Recommendations regarding the thesis:

- The relationship between the PR and the water content of tailings material should be examined. This should be done on existing TSF.
- Further research should be done to attempt and quantify the effect of local topography on the behaviour of released tailings, the run-out distance and volume released. This could be done by differentiating the existing database according to failure mechanism, total storage volume etc to refine the developed models for specific application.
- The failure database should be constantly expanded and updated to provide more datapoints for future regression studies. Regression studies play an integral role in TDBAs as a first approximation of potential risk and hazard.

6 Bibliography

Australian Government Department of Industry Tourism and Resources (2016) *Leading Practice Handbook: Tailings Management*. Australian Government Department of Industry, Tourism and Resources.

Barnston, A. G. (1992) 'Correspondence among the Correlation, RMSE, and Heidke Forecast Verification Measures; Refinement of the Heidke Score', *Weather and Forecasting*, 7, pp. 699–709.

Bian, Z. *et al.* (2012) 'The challenges of reusing mining and mineral-processing wastes', *Science*, 337(6095), pp. 702–703. doi: 10.1126/science.1224757.

Blight, G. E. (2009) *Geotechnical Engineering for Mine Waste Storage Facilities*, *Geotechnical Engineering for Mine Waste Storage Facilities*. CRC Press. doi: 10.1201/9780203859407.

Bowker, L. and Chambers, D. (2017) 'In the Dark Shadow of the Supercycle Tailings Failure Risk & Public Liability Reach All Time Highs', *Environments*, 4(4), p. 75. doi: 10.3390/environments4040075.

Bowker, L. N. *et al.* (2019) 'World Mine Tailings Failures', pp. 1–34. Available at: www.WorldMineTailingsFailures.org.

Bowker, L. N. and Chambers, D. M. (2015) *The Risk, Public Liability, & Economics of Tailings Storage Facilities Failures*.

Brumund, W. F. (1984) 'Failure of Micaceous Waste Tailings Dam', *First International Conference on Case Histories in Geotechnical Engineering*, (May), pp. 731–734.

Carmo, Flávio Fonseca do *et al.* (2017) 'Fundão tailings dam failures: the environment tragedy of the largest technological disaster of Brazilian mining in global context', *Perspectives in Ecology and Conservation*. Associação Brasileira de Ciência Ecológica e Conservação, 15(3), pp. 145–151. doi: 10.1016/j.pecon.2017.06.002.

Concha Larrauri, P. and Lall, U. (2018) 'Tailings Dams Failures: Updated Statistical Model for Discharge Volume and Runout', *Environments*, 5(2), p. 28. doi: 10.3390/environments5020028.

Coumans, C. (2002) *Introduction: Submarine Tailings Disposal, STD toolkit*.

Cunning, J. and Hawley, M. (2017) *Mine Waste Dump and Stockpile Design*. CSIRO.

Das, R. and Choudhury, I. (2013) 'Waste management in mining industry', *Indian Journal of Scientific Research*, 4(2), pp. 139–142.

Davies, M. (2011) 'Filtered dry stacked tailings: the fundamentals', *Proceedings Tailings and Mine*

Waste 2011, Vancouver B.C.

Davies, M., Martin, T. and Lighthall, P. (2000) 'Mine Tailings Dams: When Things Go Wrong', *Tailings Dams 2000*, pp. 261–274. Available at: http://citeseerx.ist.psu.edu/viewdoc/download?doi=10.1.1.597.4971&rep=rep1&type=pdf.

Dharmappa, H. B., Sivakumar, M. and Singh, R. N. (1995) 'Wastewater Minimization and Reuse in Mining Industry in lllawarra Region', pp. 11–22.

Dold, B. (2014) 'Submarine tailings disposal (STD)—A review', *Minerals*, 4(3), pp. 642–666. doi: 10.3390/min4030642.

Dubčáková, R. (2011) 'Eureqa: Software review', *Genetic Programming and Evolvable Machines*, 12(2), pp. 173–178. doi: 10.1007/s10710-010-9124-z.

Engels, J. (2004) *Risk Reduction Actions for Substandard or Impaired Tailings Facilities*, *Journal Of The West*. Available at: http://www.tailsafe.bam.de/pdf-documents/TAILSAFE_Risk_Reduction_Actions.pdf.

Geological Survey of Sweden (2019) *Mining Waste, Lecture 4*. Available at: https://www.sgu.se/en/geointro/lecture-4-mining-waste/ (Accessed: 4 December 2019).

Harraz, H. Z. (2010) 'Mine Waste Lecture'. Tanta University, (March 2010). doi: 10.13140/RG.2.1.4912.7284.

Hitch, M., Ballantyne, S. M. and Hindle, S. R. (2010) 'Revaluing mine waste rock for carbon capture and storage', *International Journal of Mining, Reclamation and Environment*, 24(1), pp. 64–79. doi: 10.1080/17480930902843102.

Holmqvist, M. and Gunnteg, M. (2014) *Seepage , Solute transport and Strain-stress Analysis of Ashele Tailings Dams*. Uppsala Universitet.

ICOLD (2001) *Tailings Dams: Risk of Dangerous Occurrences, ICOLD Committee on Tailings Dams and Waste Lagoons*.

International Council on Mining & Metals (2020) *Global Industry Standard on Tailings Management*.

Kalin, M. (2004) 'Passive mine water treatment: The correct approach?', *Ecological Engineering*, 22(4–5), pp. 299–304. doi: 10.1016/j.ecoleng.2004.06.008.

Kheirkhah Gildeh, H. *et al.* (2020) 'Tailings Dam Breach Analysis: A Review of Methods, Practices, and Uncertainties', *Mine Water and the Environment*. Springer Berlin Heidelberg, (Cda 2013). doi:

10.1007/s10230-020-00718-2.

Klohn Crippen Berger (2017) *Study of Tailings Management Technologies*. Available at: http://mend-nedem.org/wp-content/uploads/2.50.1Tailings_Management_TechnologiesL.pdf.

Kossoff, D. *et al.* (2014) 'Mine tailings dams: Characteristics, failure, environmental impacts, and remediation', *Applied Geochemistry*. Elsevier Ltd, 51, pp. 229–245. doi: 10.1016/j.apgeochem.2014.09.010.

Lefebvre, R. (1995) 'Modeling acid mine drainage in waste rock dumps', in *TOUGH Workshop '95*, pp. 239–244.

Li, A. *et al.* (2009) 'Stability of Large Thickened, Non-Segregated Tailings Slopes', *Proceedings of the Twelfth International Seminar on Paste and Thickened Tailings*, pp. 301–311. doi: 10.36487/acg_repo/963_34.

Marais, N. (2019) 'Breach volume predictions: The consequences of tailings malpractice', in *SAIMM Mineral Research Conference*.

Martin, V., Al-Mamun, M. and Small, A. (2019) 'CDA technical bulletin on tailings dam breach analyses', *Sustainable and Safe Dams Around the World*, d, pp. 3484–3498. doi: 10.1201/9780429319778-313.

Mohapatra, D. P. and Kirpalani, D. M. (2017) 'Process effluents and mine tailings: sources, effects and management and role of nanotechnology', *Nanotechnology for Environmental Engineering*. Springer International Publishing, 2(1), pp. 1–12. doi: 10.1007/s41204-016-0011-6.

Owen, J. R. *et al.* (2020) 'Catastrophic tailings dam failures and disaster risk disclosure', *International Journal of Disaster Risk Reduction*, 42. doi: 10.1016/j.ijdrr.2019.101361.

Pacheco, R. L. R. (2019) 'Static liquefaction in tailings dam and flow failure', (February).

Quelopana, H. (2019) 'Released Volume Estimation for Dam Break Analysis', in *Tailings Management 2019*, pp. 1–12.

Rico, M., Benito, G., Diez-Herrero, A., *et al.* (2008) 'Floods from Tailings Dam Failures', *Spanish Geological Survey (IGME)*, 154(1–3), pp. 1–22. doi: 10.1016/j.jhazmat.2007.09.110.

Rico, M., Benito, G., Salgueiro, A. R., *et al.* (2008) 'Reported tailings dam failures. A review of the European incidents in the worldwide context', *Journal of Hazardous Materials*, 152(2), pp. 846–852. doi: 10.1016/j.jhazmat.2007.07.050.

Roca, M., Murphy, A. and Vallesi, S. (2019) *A review of the risks posed by the failure of tailings dams*.

Roche, C., Thygesen, K. and Baker, E. (2017) *Mine Tailings Storage: Safety Is No Accident. UNEP Rapid Response Assessment. United Nations Environment Programme*. Available at: https://gridarendal-website-live.s3.amazonaws.com/production/documents/:s_document/371/original/RRA_MineTailings_lores.pdf?1510660693.

Rourke, H. and Luppnow, D. (2015) 'The risks of excess water on tailings facilities and its application to dam-break studies', *Tailings and Mine Waste Management for the 21st Century*, (July), pp. 225–230.

Sarsby, R. (2000) *Environmental Geotechnics*. Thomas Telford Publishing.

U.S Environmental Protection Agency (1994) 'Design and Evaluation of Tailings Dams', *U.S. Environmental Protection Agency, Office of Solid Waste, Speacial Waste Branch*, (August), pp. 5–14. doi: EPA 530-R-94-038.

UNEP and Mining Journal Research Services (1996) *Environmental and Safety Incidents concerning Tailings Dams at Mines*.

Vick, S. G. (1990) *Design, Planning and Analysis of Tailings Dams*. John Wiley & Sons.

7 Appendices

7.1 Appendix A.1: Process flow diagram of TDBAs

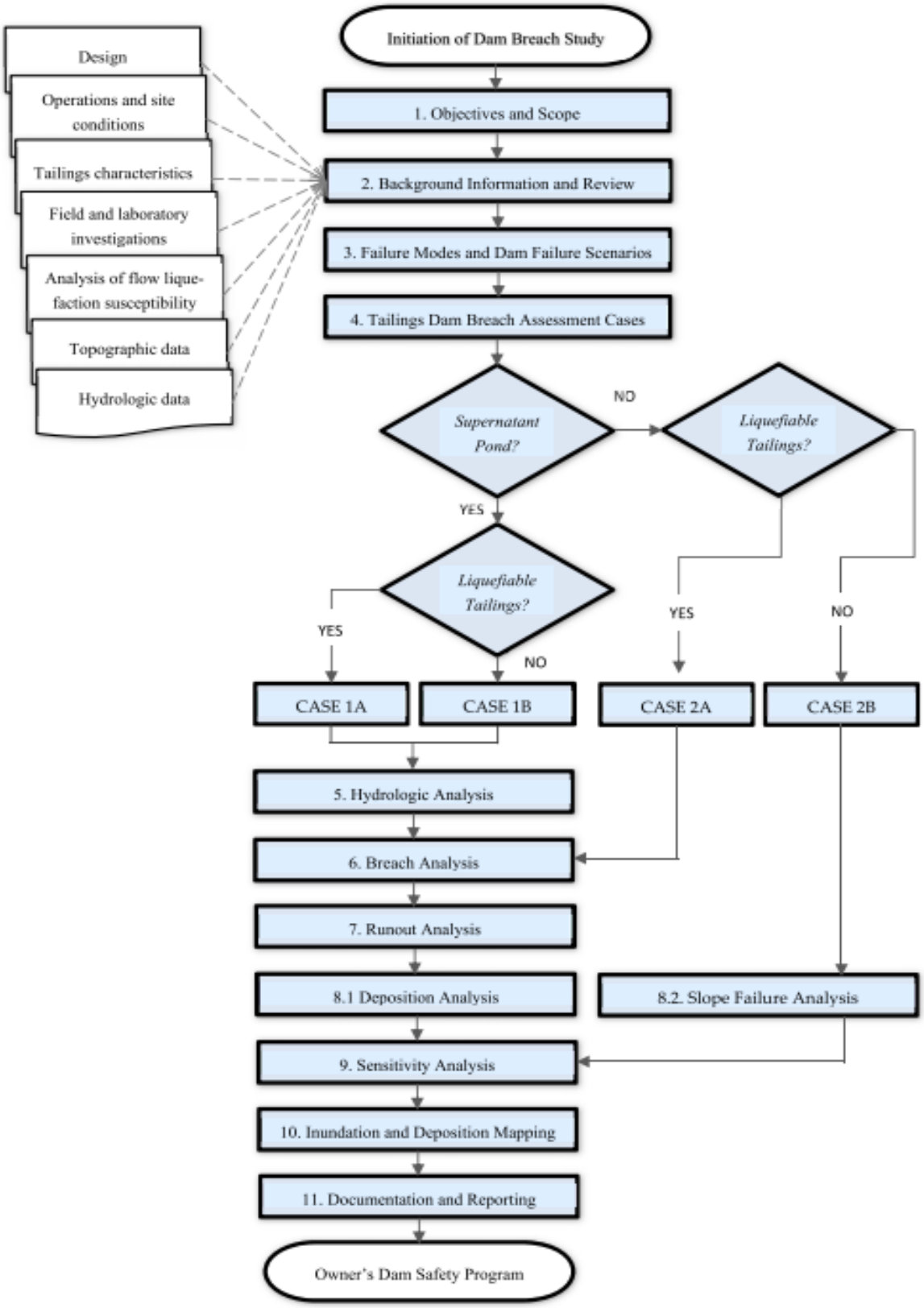

7.2 Appendix B.1: Rico et al (2008) Failure Database

Ref. Nº.	Name of the Dam	Date of failure (year)	Type of dam	Dam Height (m)	Impoudment volume ($x10^6 m^3$)	Run-out Distance (km)	Dam Factor (HxV_F)	Released Volume ($x10^6 m^3$)
1	Arcturus (Zimbawe)	1978	RING	25	1.7-2.0 Mt	0.3	0.5	0.0211
2	Bafokeng (South Africa)	1974	RING	20	13	45	60	3
3	Baia Mare (Romania)	2000	UPS	7	0.8	0.18	0.7	0.1
4	Bellavista (Chile)	1965	RING	20	0.45	0.8	1.4	0.07
5	Buffalo Creek (USA)	1972	UPS	14-18	0.5	64.4	7-9	0.5
6	Cerro Negro No.3 (Chile)	1965	UPS	20	0.5	5	1.7	0.085
7	Cerro Negro No.4 (Chile)	1985	MXSQ	40	2	8	20	0.5
8	Churchrock (USA)	1979	WR	11	0.37	96.5-112.6	4.07	0.37
9	Cities Service (USA)	1971	WR	15	12.34	120	135	9
10	El Cobre Old Dam (Chile)	1965	UPS	35	4.25	12	66.5	1.9
11	Galena Mine (USA)	1974	UPS	9		0.61	0.034	0.0038
12	Gypsum Tailings Dam (USA)	1966	UPS	11	7 Mt	0.3	0.88-1.43	$2 x10^5 t$
13	Hokkaido (Japan)	1968	UPS	12	0.3	0.15	1.08	0.09
14	Itabirito (Brazil)	1986	Gravity	30		12	3	0.1
15	La Patagua New Dam (Chile)	1965	RING	15		5	0.525	0.035
16	Los Frailes (Spain)	1998	RING	27	15-20	41	53.51	4.6
17	Los Maquis (Chile)	1965	UPS	15	0.043	5	0.315	0.021
18	Merriespruit (South Africa)	1994	RING	31	7.04	2	18.6	2.5 Mt
19	Mochikoshi No.1 (Japan)	1978	UPS	28	0.48	8	2.24	0.08
20	Mochikoshi No.2 (Japan)	1978	UPS	19		0.15	0.057	0.003
21	Ollinghouse (USA)	1985	WR	5	0.12	1.5	0.125	0.025
22	Omai (Guyana)	1995	WR	44	5.25	80	184.8	4.2
23	Phelps-Dodge (USA)	1980	UPS	66	2.5	8	132	2
24	Sgurigrad (Bulgaria)	1966	UPS	45	1.52	6	9.9	0.22
25	Stancil (USA)	1989	UPS	9	0.074	0.1	0.342	0.038
26	Stava (Italy)	1985	RING	29.5	0.3	4.2	5.605	0.19
27	Tapo Canyon (USA)	1994	UPS	24		0.18		
28	Unidentified (USA)	1973	UPS	43	0.5	25	7.31	0.17
29	Veta del Agua Nº1 (Chile)	1985	MXSQ	24	0.7	5	6.72	0.28

7.3 Appendix B.2: Concha Larrauri & Lall (2018) Failure Database

No	Mine	Year	H (m)	V_T ($\times 10^6$ m^3)	D_{max} (km)	V_F ($\times 10^6$ m^3)	Failure Type [a]	Source
1	(unidentified), Southwestern USA	1973	43	0.5	25	0.17	SI	Rico
2	Aitik mine, Sweden (Boliden Ltd.)	2000	15	15	5.2	1.8	ER	CB
3	**Arcturus (Zimbawe)**	**1978**	**25**	**1.7–2 Mt**	**0.3**	**0.0211** [b]	**OT**	**Rico**
4	Bafokeng, South Africa	1974	20	13 [c]	45	3	SE	Rico
5	Balka Chuficheva, Russia	1981	25	27	1.3	3.5	SI	CB
6	Bellavista, Chile	1965	20	0.45	0.8	0.07	EQ	Rico
7	Bonsal, North Carolina, USA	1985	6	0.038	0.8	0.011	OT	CB
8	Cerro Negro No. (3 of 5)	1965	20	0.5	5	0.085	EQ	Rico
9	Cerro Negro No. (4 of 5)	1985	40	2	8	0.5	EQ	Rico
10	Churchrock, New Mexico, United Nuclear	1979	11	0.37	110 [d]	0.37	FN	Rico/CB
11	Cities Service, Fort Meade, Florida	1971	15	12.34	120	9	SE	Rico
12	Deneen Mica Yancey County, North Carolina, USA	1974	18	0.3	0.03	0.038	SI	CB
13	El Cobre New Dam	1965	19	0.35	12	0.35	EQ	CB
14	El Cobre Old Dam	1965	35	4.25	12	1.9	EQ	Rico
15	Fundão-Santarem, Minas Gerais, Brazil (Samarco)	2015	90	55	637	32 [e]	ST	CB
16	**Galena Mine (1974)**	**1974**	**9**	**NA**	**0.61**	**0.0038**	**OT**	**Rico**
17	**Gypsum Tailings Dam (Texas, USA)**	**1966**	**11**	**7** [f]	**0.3**	**0.085**	**SE**	**CB**
18	Hokkaido, Japan	1968	12	0.3	0.15	0.09	EQ	Rico
19	Imperial Metals, Mt Polley, British Columbia, Canada	2014	40	74	7	23.6	FN	CB
20	**Itabirito (Brazil)**	**1986**	**30**	**NA**	**12**	**0.1**	**ST**	**Rico**
21	**La Patagua New Dam (Chile)**	**1965**	**15**	**NA**	**5**	**0.035**	**EQ**	**Rico**
22	Los Frailes, near Seville, Spain (Boliden Ltd.)	1998	27	15	41	6.8 [g]	FN	CB
23	Los Maquis No. 3	1965	15	0.043	5	0.021	EQ	Rico
24	Merriespruit, South Africa (Harmony)-No. 4A Tailings Complex	1994	31	7.04	4 [h]	0.6 [h]	OT	CB
25	Mochikoshi No. 1, Japan (1 of 2)	1978	28	0.48	8	0.08	EQ	Rico
26	**Mochikoshi No. 2 (Japan)**	**1978**	**19**	**NA**	**0.15**	**0.003**	**EQ**	**Rico**
27	Olinghouse, Nevada, USA	1985	5	0.12	1.5	0.025	SE	Rico
28	Omai Mine, No. 1, 2, Guyana (Cambior)	1995	44	5.25	80	4.2	ER	Rico
29	Prestavel Mine-Stava, North Italy, 2, 3 (Prealpi Mineraria)	1985	29.5	0.3	8 [i]	0.2	SI	Rico
30	Sgurigrad, Bulgaria	1996	45	1.52	6	0.22	SI	Rico
31	Stancil, Maryland, USA	1989	9	0.074	0.1	0.038	SI	Rico
32	Taoshi, Linfen City, Shanxi province, China (Tahsan Mining Co.)	2008	50.7	0.29	2.5	0.19	U	CB
33	**Tapo Canyon (USA)**	**1994**	**24**	**NA**	**0.18**	**NA**	**EQ**	**Rico**
34	Tyrone, New Mexico (Phelps Dodge)	1980	66	2.5	8	2	SI	Rico
35	Veta de Agua (Chile)	1985	24	0.7	5	0.28	EQ	Rico

[a] SI = Slope instability, EQ = Earthquake, OT = Overtopping, ER = Erosion, FN = Foundation, SE = Seepage, U = Undefined. [b] CB report 0.039 $\times$ 10^6 m^3 V_F. [c] In Rico 13 $\times$ 10^6 m^3 as [16] and [17]; in CB 17 $\times$ 10^6 m^3. [d] In CB 110 km as in [18] and [17], in Rico 96.5–112.6 km. [e] 43 $\times$ 10^6 m^3 in [19]. [f] Rico in tones. [g] In Rico 4.6 $\times$ 10^6 m^3; in [20] 10^6 m^3, in [21] 5.5 $\times$ 10^6 m^3 of tailings and 1.9 $\times$ 10^6 m^3 of acid water; in [17] 5.5 Mm^3. [h] In Rico 2.5 Mt V_F and 2 km in D_{max} as in [22]; in [5] 0.6 $\times$ 10^6 m^3. [i] In Rico 4.2 km D_{max}; in [13] 8 km.

7.4 Appendix B.3: Quelopana (2019) Failure Database

No	Mine/Deposit	Country	Year	Dam	Failure	VR Mm³	VT Mm³	H m	VR/VT
1	Arcturus (U)	Zimbawe	1978	US-T	SI	0.07	0.68	25	0.10
2	Bafokeng	South Africa	1974	US-T	SE	3.00	13.00	20	0.23
3	Balka Chuficheva	Russia	1981	US-CS	SI	3.50	27.00	25	0.13
4	Barahona (N)	Chile	1928	US-CS	EQ	2.80	20.00	65	0.14
5	Bellavista (U)	Chile	1965	US-T	EQ	0.07	0.21	20	0.34
6	Brumadinho (N)	Brasil	2019	US-T	UN	9.57	11.96	87	0.80
7	Cerro Negro No3 (U)	Chile	1965	US-T	EQ	0.09	0.26	20	0.33
8	Cerro Negro No4 (U)	Chile	1985	US-CS	EQ	0.09	1.05	33	0.09
9	Deneen Mica	USA	1974	US-CS	SI	0.04	0.30	18	0.13
10	El Cobre New Dam (U)	Chile	1965	UN-CS	EQ	0.50	0.50	19	1.00
11	El Cobre Old Dam	Chile	1965	US-T	EQ	1.90	4.25	35	0.45
12	Fundao (U)	Brasil	2015	US-T	SI	32.00	55.00	110	0.58
13	Gypsum Tailings Dam (U)	USA	1966	US-T	SE	0.14	5.00	11	0.03
14	Hokkaido (U)	Japan	1968	US-T	EQ	0.09	0.30	9	0.30
15	Huogudu (N)	China	1962	US-UN	UN	3.30	5.42	19	0.61
16	Kolontar (N)	Hungary	2010	DS-F	SI	0.65	4.20	22	0.15
17	La Luciana (N)	Spain	1960	US-T	SI	0.25	1.25	24	0.20
18	Las Palmas (N)	Chile	2010	DS-CS	EQ	0.17	0.22	15	0.80
19	Los Cedros (N)	Mexico	1937	US-T	SI	2.50	11.48	35	0.22
20	Los Frailes (U)	Spain	1998	DS-E	FN	2.00	17.50	27	0.11
21	Los Maquis No3 (U)	Chile	1965	US-T	EQ	0.02	0.03	15	0.82
22	Merriespruit (U)	South Africa	1994	US-T	OT	0.55	7.04	25	0.08
23	Mike Horse (N)	USA	1975	US-T	OT	0.07	0.25	18	0.29
24	Mochikoshi No1	Japan	1978	US-T	EQ	0.08	0.48	28	0.17
25	Mount Polley (U)	Canada	2014	CL-E	FN	13.40	63.40	40	0.21
26	Niujialong (N)	China	1985	US-UN	OT	0.73	1.10	40	0.66
27	Olinghouse	USA	1985	WR-E	SE	0.03	0.12	5	0.21
28	Sgurigrad	Bulgaria	1966	US-T	SI	0.22	1.52	45	0.14
29	Silver King (N)	USA	1974	DS-E	OT	0.01	0.04	9	0.16
30	Stancil	USA	1989	US-E	SI	0.04	0.07	9	0.51
31	Stava (U)	Italy	1985	US-CS	SI	0.20	0.30	28	0.68
32	Unidentified	USA	1973	US-E	SI	0.17	0.50	43	0.34
33	Veta del Agua No5 (N)	Chile	2010	US-CS	EQ	0.03	0.08	16	0.34
34	Xiangfen	China	2008	US-T	SI	0.19	0.29	51	0.66
35	Zlevoto No4 (N)	Yugoslavia	1976	US-T	SI	0.30	1.00	25	0.30
	Average	--	--	--	--	**2.25**	**7.31**	**30**	**0.35**

(U) Updated data; (N) New case; Dam type: (US) Upstream, (CL) Center line, (DS) Downstream, (WR) Water retention, (T) Tailings, (CS) Sand Tailings, (E) Earthfill or Rockfill, (F) Fly Ash, (UN) Unknown; Failure type: (SI) Slope instability, (SE) Seepage, (FN) Foundation, (OT) Overtopping, (EQ) Earthquake, (UN) Unknown

7.5 Appendix B.4: Rourke & Luppnow (2015) Failure Database

Name	Impoundment storage volume (Mm^3)	Release volume (m^3)	Ratio of release volume to stored volume (%)	Ratio of pool area to total area (%)
Merriespruit	7.0	0.6	9	14
Bafokeng	13.0	3.0	23	30
Mount Polley	50.0	24.4	49	72
Kolontár	1.2	0.7	58	88
Stava	0.3	0.2	67	100

7.6 Appendix C.1

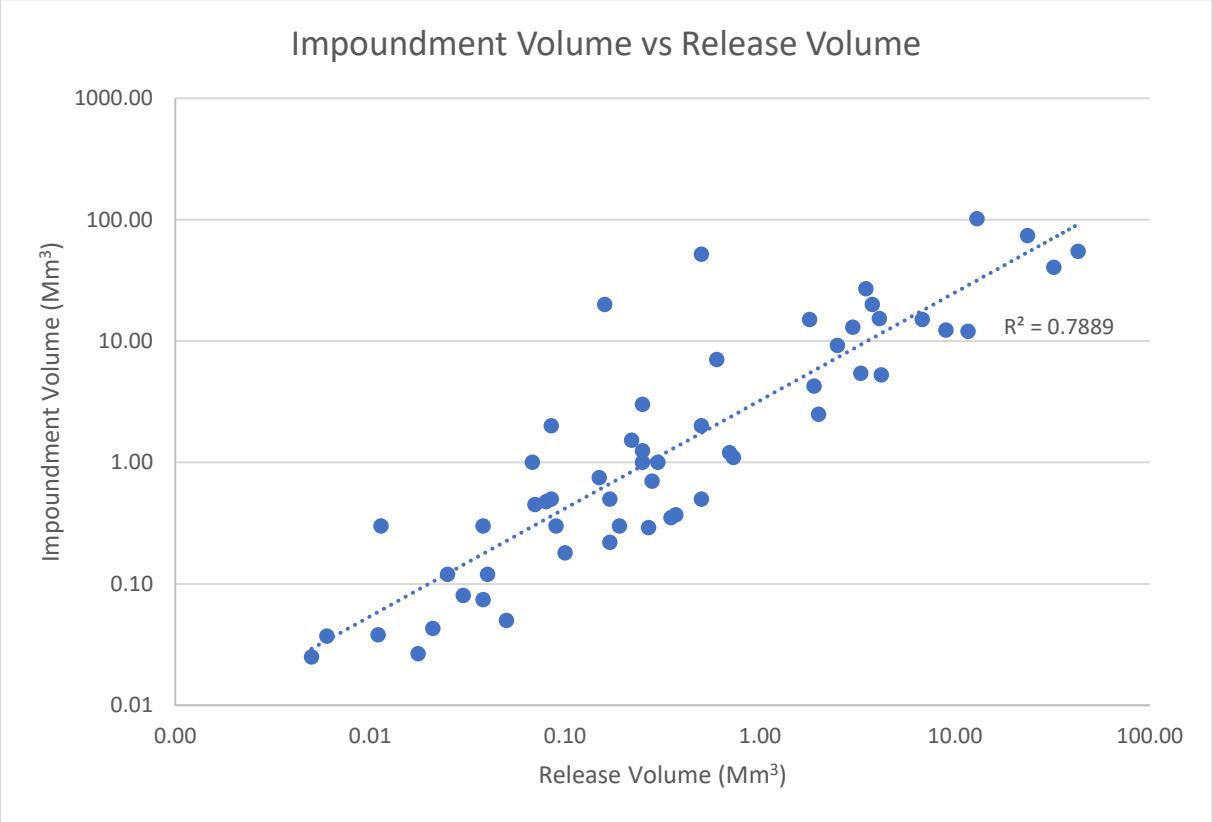

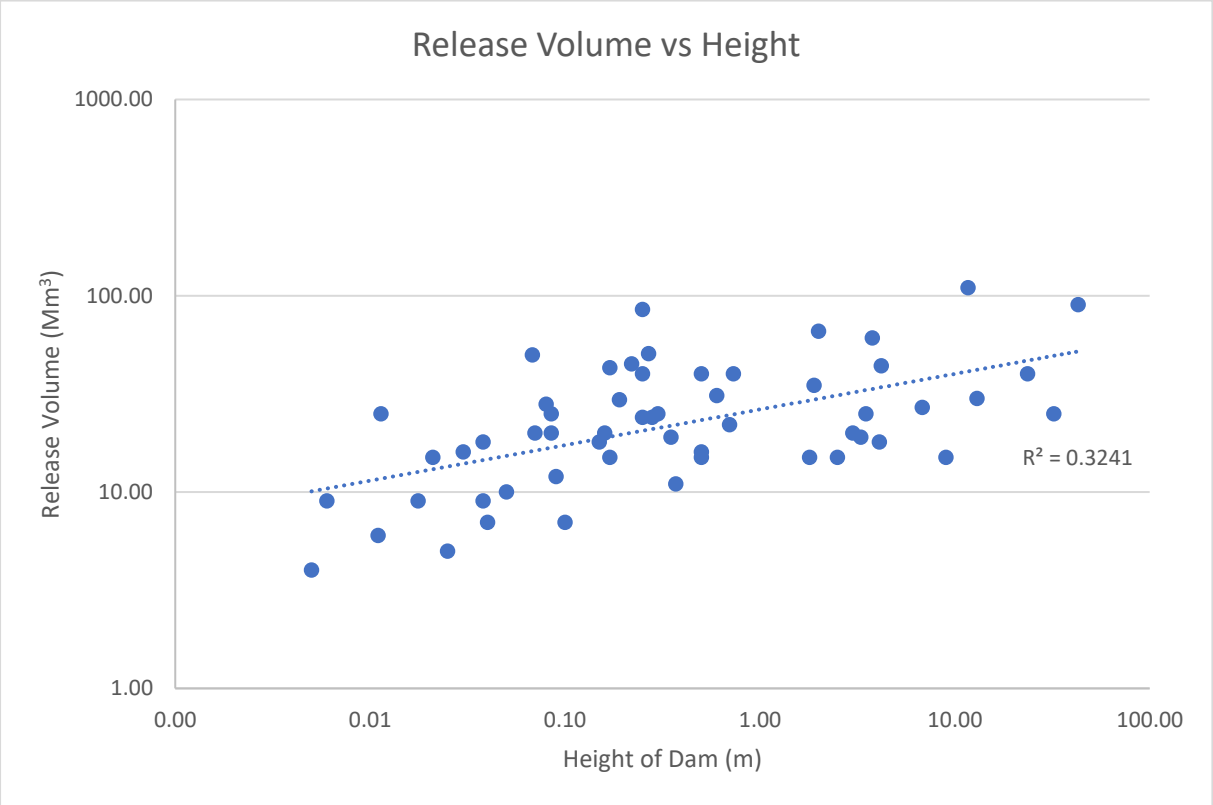

7.7 Appendix C.2